

# Preservation Potential of Permian Gypsum Beds, Nippewalla Group, USA

By

Dru Lockamy

B.S., Wichita State University, 2014

Submitted to the graduate degree program in Geology and the Graduate Faculty of the University of Kansas in partial fulfillment of the requirements for the degree of Master of Science.

---

Alison Olcott Marshall, Chair

---

Doug Walker

---

Diane Kamola

Date Defended: 04/09/2018

The Thesis Committee for Dru Lockamy  
certifies that this is the approved version of the following thesis:

Preservation Potential of Permian Gypsum Beds, Nippewalla Group, USA

---

Alison Olcott Marshall, Chairperson

Date Approved: 04/09/18

## ABSTRACT

During the Permian, what is now southern Kansas and northern Oklahoma was a drying inhospitable environment, as evidenced by the extensive red-beds and evaporites of the Nippewalla Group. Due to the fact that animals could not live in much of this extreme environment, there is a lack of a traditional fossil record in these units. Thus, this study focuses on detecting biomarkers, the chemical traces of organisms. The red-beds and gypsum were analyzed in order to assess their biomarker contents. Geochemistry similar to that found in the Nippewalla Group has been hypothesized to prevent the preservation of biomarkers due to the presence of hematite, which indicates oxidizing conditions. Due to these circumstances, a series of methods were used to investigate the detection of biomarkers. Thin sections of each rock and mineral sample, as well as two thick sections, were prepared in order to investigate the presence of fluid inclusions and any preserved organic matter through the use of fluorescence microscopy. The extractable organic matter and the total organic carbon (TOC) were also analyzed, allowing for the identification of *n*-alkanes, hopanes, methyl-hopanes, nor-hopanes, and isoprenoids, pristane and phytane, mostly within the gypsum.

The presence of these biomarkers indicate that they can be preserved in oxidizing conditions, at least in the presence of gypsum, as it is likely the key factor to the biomarkers sustainability. The gypsum contained a number of fluid inclusions where organic material could be preserved. Also, the gypsum could create microenvironments and provide a barrier between the surrounding oxic environment and the inner anoxic environment.

Understanding the preservation potential of gypsum is important as biomarkers can provide paleoenvironmental insight into the environmental conditions of the Permian. They can also provide clues to possible preservation pathways within the gypsum on Mars as the

paleoenvironment of the Nippewalla Group was similar to the environment on Mars based on mineralogy and sedimentology.

## **Acknowledgements**

I would like to thank the University of Kansas Geology Department and my advisor, Alison Olcott Marshall, for accepting me into their program and allowing me to further my education. Since arriving at KU I have felt at home and couldn't think of another place I would rather pursue my higher education. It was with the support of Alison, my committee members Craig Marshall, and Diane Kamola, and other faculty and staff at KU, that I was able to accomplish my goals in order to obtain my masters of science degree in geology. My friends and colleagues that I acquired during my time spent in classrooms or studying were also a great source of encouragement and enlightenment. I would also like to thank my wife, Kayly Lockamy, without her support I couldn't have accomplished this goal.

## TABLE OF CONTENTS

<b>ABSTRACT</b> .....	<b>iii</b>
<b>Acknowledgements</b> .....	<b>v</b>
<b>CHAPTER ONE: Introduction</b> .....	<b>1</b>
<b>1.1 Introduction</b> .....	<b>1</b>
<b>1.2 Geologic Background</b> .....	<b>3</b>
<b>1.3 Biomarkers</b> .....	<b>7</b>
<b>1.4 Fluid Inclusions</b> .....	<b>15</b>
<b>CHAPTER TWO: Sample Collection and Methods</b> .....	<b>17</b>
<b>2.1 Field Site</b> .....	<b>17</b>
<b>2.2 Sample Collection</b> .....	<b>19</b>
<b>2.3 Sample Preparation</b> .....	<b>20</b>
<b>2.3.1 Solvent Extraction</b> .....	<b>21</b>
<b>2.3.2 GCMS Analysis</b> .....	<b>22</b>
<b>2.4 Analysis of TOC</b> .....	<b>23</b>
<b>2.5 Thin Section Analysis</b> .....	<b>24</b>
<b>CHAPTER THREE: Results</b>	
<b>3.1 Organic Matter Content</b> .....	<b>25</b>
<b>3.2 Co-elution</b> .....	<b>25</b>
<b>3.3 Biomarker Analysis</b> .....	<b>25</b>
<b>3.3.1 Hopanes</b> .....	<b>25</b>
<b>3.3.2 <i>n</i>-Alkanes</b> .....	<b>30</b>
<b>3.4 TOC Analysis</b> .....	<b>35</b>
<b>3.5 Thin Section Analysis</b> .....	<b>35</b>
<b>CHAPTER FOUR: Discussion</b> .....	<b>41</b>
<b>4.1 Modern Contaminants</b> .....	<b>41</b>
<b>4.2 <i>n</i>-Alkane Interpretation</b> .....	<b>43</b>
<b>4.3 Hopane Interpretation</b> .....	<b>46</b>
<b>4.4 Geochemistry of the Nippewalla Group</b> .....	<b>47</b>
<b>4.5 Microenvironments</b> .....	<b>48</b>
<b>4.6 Fluid Inclusions</b> .....	<b>50</b>
<b>4.7 Mars</b> .....	<b>51</b>

**CHAPTER FIVE: Conclusion.....53**  
**References.....54**

## CHAPTER ONE

### 1.1 Introduction

The Nippewalla Group, extending from southern Kansas to northern Oklahoma, contains extensive Permian red-beds and evaporites consisting of halite, anhydrite, and gypsum (Benison, 1997; Benison and Goldstein, 2001). Within these red-beds and evaporites the traditional fossil record is scarce, with only invertebrate fossils discovered in a thin dolostone bed of the Blaine Formation in southern Oklahoma (Foster et al., 2014; Sweet et al., 2013). The rarity of traditional fossils is due to the drying inhospitable environment, indicated by the evaporites associated with the red-beds present at the time of deposition, and also the extreme acidity of the Permian waters in the Nippewalla Group (Benison et al., 1998).

These red-beds are shown to be primary and have an eolian origin from the Appalachian – Ouachita orogen, evidenced by the fine and uniform grain size, along with massive bed structures (Foster et al., 2014; Sweet et al., 2013). This evidence shows that the red-beds were deposited as a loess in an episodically wet environment (Foster et al., 2014). The gypsum is also shown to be primary, which can be indicated by the presence of iron-oxide found throughout the gypsum and other relationships with the associated anhydrite as outlined in McGregor, (1948). The primary origin of the red-beds and gypsum is important. As it would show that if any fossils were discovered in the Nippewalla Group the animal or organism they belonged to, possibly lived in this environment.

Hematite is one of the main constituents of the red-beds, indicating oxidizing conditions, and it has been hypothesized that the redox conditions of the Nippewalla Group red-beds would result in poor preservation of any organism that must have lived in these sediments during the

Permian (Sumner, 2004). Oxidizing environments often lead to degradation of organisms instead of preservation. However, the preservation of such organisms is important, as their preserved counterparts, biomarkers, can indicate the type of organism present during rock formation. These biomarkers, defined as compounds derived from lipids, in most cases, can be traced back to a particular biological precursor molecule (Killops and Killops, 2005). Therefore, they are able to provide evidence of the paleoenvironment and allow insight into their preservation as well.

To date there have been no biomarker studies of iron-rich rock beds and evaporites from the same lithostratigraphic unit to test the preservation potential of the evaporites, nor whether the conclusions of the Sumner (2004) model are apparent in these rocks. However, other studies of organic matter and microfossil preservation from correlative Permian units and evaporites of younger rock units have yielded promising results. Researchers have discovered evidence of fossilized organic-walled microbial life in bottom-nucleated gypsum in correlative Permian units of the Seven Rivers Formation and the Salado Formation in New Mexico (Schopf et al., 2012). The microfossils were detected with the use of transmitted white light optical microscopy, plane polarized light optical microscopy, confocal laser scanning microscopy, and Raman spectroscopy (Schopf et al., 2012). Another study conducted on the Opeche Shale Formation in North Dakota found hairy blobs in cored halite (Benison et al., 2008). These hairy blobs were identified as bodies of unusual characteristics, consisting of sulfate crystals and organic matter that may represent some form of microbial remains, and were detected with the aid of plane-light, reflected-light, and polarized-light petrography, fluorescence microscopy, scanning electron microscopy, and Raman spectroscopy (Benison et al., 2008). Another geologic study identified preserved sulfurized biomarkers in marls found in evaporite sequences in the Messinian evaporitic basin in northern Italy (Damste et al., 1986). This study used a gas chromatograph

equipped with a flame photometric detector (GC-FPD) and a gas chromatograph mass spectrometer (GCMS). The composition of molecular structures and lipid biomarkers of a modern endoevaporitic gypsarenite microbial mat community were investigated and identified as short – chain fatty acids and hopanoids up to C<sub>32</sub>, using a GCMS (Jahnke et al., 2014). Results from these studies suggest that the gypsum beds of the Nippewalla Group could contain signs of life, despite what the redox conditions suggest, by presenting geological and modern evidence of their preservation.

This study of the Nippewalla Group will focus on the extractable organic compounds preserved in gypsum and the surrounding rock. Analyzing these factors will help gain meaningful insight into how biomarkers are preserved and will help refine depositional conditions of the Nippewalla Group.

## **1.2 Geologic Background**

Strata of the Nippewalla Group, along with other siliciclastic red-beds and evaporites located in the Midcontinent of North America (Soreghan et al., 2014), are bounded by arches, anticlines, and areas of uplift (Benison, 1997; Benison and Goldstein, 2001). These structural features formed the boundaries of the mid-Permian depositional basins. The Las Animas Arch and the Nemaha Anticline trend north and south, bordering the western and eastern extents of the Permian red beds and evaporites, respectively. As the formation of Pangea was coming to an end during the Leonardian Series of the Mid-Permian (Baars, 1990), the Nippewalla Group was deposited in a series of these basins, which include the Hugoton Embayment of the Anadarko Basin, and the Sedgwick, Syracuse, and Cimarron basins (Benison, 1997; Benison and Goldstein, 2001). The Syracuse Basin extends throughout the western region of the red bed and

evaporite deposition. The eastern extent of deposition occurs in the Sedgwick Basin and the southern extent within the Hugoton Embayment of the Anadarko Basin. Located between the Syracuse and Sedgwick Basins is the Cimarron Basin (Figure 1.1) (Giles et al., 2013).

The Nippewalla Group (Figure 1.2) contains the Dog Creek Formation, Blaine Formation, Flowerpot Shale, Cedar Hills Sandstone, Salt Plain Formation, and the Harper Sandstone (Benison, 1997; Benison and Goldstein, 2001; Sweet et al., 2013). Red-bedded siliciclastic sandstone, siltstone, and mudstone are the dominant lithologies in surface exposures (Benison, 1997; Benison and Goldstein, 2001). Hematite is prevalent in the Nippewalla Group

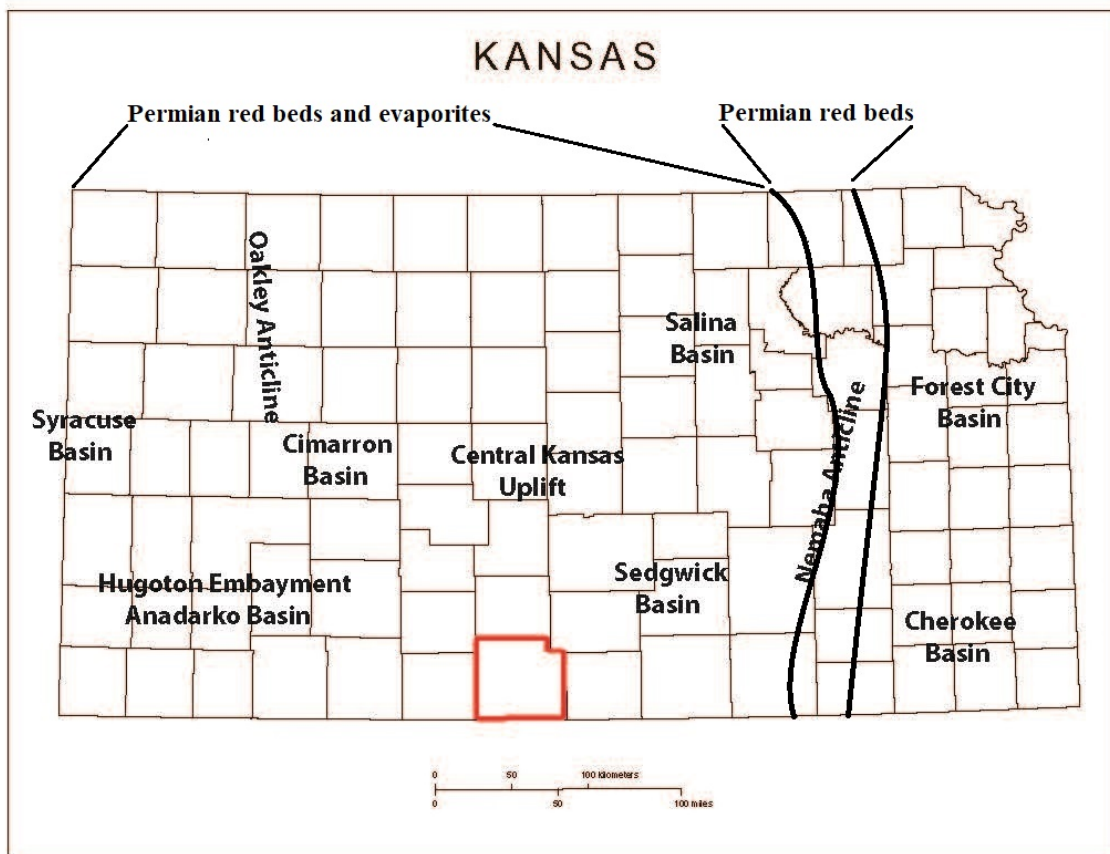


**Figure 1.1** Map of Kansas showing depositional basins, structural features, and the extent of deposition of Permian red-beds and red-beds with evaporites after (Benison et al., 2015; Holdaway, 1978; Newell et al., 1989). – Barber County is highlighted in red.

and coats many of the grains within the rock sequence (Benison, 1997). Evaporites such as gypsum and anhydrite are also present. The Dog Creek, Blaine, and Flowerpot Shale formations contain significant amounts of gypsum and/or anhydrite and are the main focus of this study, as these types of evaporites are the main target for biomarker preservation.

Correlations between subsurface and surface expressions of the Nippewalla Group are difficult, because of surficial dissolution of halite and nomenclatural differences in Kansas and Oklahoma (Benison et al., 2015; Holdaway, 1978). Strat of interest are called the Nippewalla Group in Kansas and the El Reno Group in Oklahoma. For the purpose of this study, the nomenclature Nippewalla Group will be used throughout. Thicknesses of the Nippewalla Group have ranged from approximately 152 meters to 284 meters at the surface, while subsurface lithologies have been estimated at 150 meters (Benison and Goldstein, 2001; Benison et al., 2015; Holdaway, 1978). Cores were used to determine the lithologies of the formations in the subsurface while outcrop observations were used for surficial exposures (Benison and Goldstein, 2001). With the exception of the Blaine Formation, all formations consist of one or more of the following lithologies in varying concentrations (Figure 1.2): red mudstone, red sandstone, gray/red siltstone and shale. The Blaine Formation consists only of gypsum and anhydrite. In the subsurface, all formations also contain either bedded halite or displacive halite (Benison, 1997; Benison and Goldstein, 2001; Benison et al., 2015; Giles et al., 2013; Johnson, 1967).

This study will focus on the three formations previously mentioned. These formations were described to contain the highest amounts of gypsum or anhydrite and were targeted on the notion that they may contain preserved biomarkers.

PERMIAN	OCHOAN	 missing strata	dominant lithologies in surface exposures	depositional environment	samples	
	GUADALUPIAN		Big Basin Formation			red siltstones, sandstones
			Day Creek Dolomite			anhydrite, grey shales
			Whitehorse Formation			pink sandstones
	LEONARDIAN	NIPPEWALLA GROUP	<b>Dog Creek Formation</b>	red mudstones, siltstones, anhydrite	eolian shallow water environment	DCSS#1, DC#2, DC#3
			<b>Blaine Formation</b>	anhydrite, gypsum	saline lake environment	CG#1, GG#1
			<b>Flowerpot Shale</b>	red mudstones, siltstones, anhydrite	perennial lake and dry mudflat environment	FSG#1, SP#1, FPA#1, FP#1
		SUMNER GROUP	<b>Cedar Hills Sandstone</b>	red siltstones, sandstones		
			<b>Salt Plain Formation</b>	red mudstones, siltstones, anhydrite		
			<b>Harper Sandstone</b>	red siltstones, sandstones		
Stone Corral Formation			anhydrite			
		Ninnescah Shale	red mudstones			
		Wellington Formation	grey shales			

**Figure 1.2:** Description and stratigraphic relation of the Nippewalla Group including sample identifications (modified from Benison and Goldstein, 2001). The Dog Creek, Blaine, and Flowerpot Shale formations were studied for biomarker preservation.

### **1.3 Biomarkers**

Some depositional environments are too harsh for animals or other macroscopic organisms to inhabit. These extreme conditions can include, but are not limited to, high temperatures, high acidity, and high salinity (Majhi et al., 2013; Rothschild and Mancinelli, 2001; Schafer, 2004). Some extremophilic Bacteria and Archaea, however, are able to thrive under these conditions due to their unique adaptations and the lack of predation in these environments. If microbes are preserved in the Nippewalla Group they would be considered extremophiles, because the waters present during deposition of the Nippewalla Group were extremely acidic (Benison et al., 1998). Also, the siliciclastics (red-beds) are associated with evaporites, providing evidence for oxidizing environmental conditions during the time of rock deposition. These environmental conditions are not favorable to the preservation of microbes (Sumner, 2004). Under the right environmental conditions, however, microbes can be preserved. Once they are preserved they are subjected to diagenesis, which alters them chemically and leaves their chemical remnants (biomarkers) behind. Biomarkers are lipid-derived chemical fossils originating from organisms present during deposition of the surrounding rock (Gelpi et al., 1970; Killops and Killops, 2005; Peters et al., 2005b). They can be difficult to preserve, with preservation dependent upon environmental conditions of the depositional setting.

Preservation of biomarkers is affected by numerous factors. These factors include the quantity of organic matter present during deposition, grain size, and whether the environment is oxic or anoxic. Organic matter preferentially accumulates in low-energy settings (Killops and Killops, 2005). Grain size can play an important role in the preservation of organic material as fine-grained sediments, usually mud or silt, exclude oxygen-rich water more readily, enabling better preservation (Peters et al., 2005b; Sumner, 2004). In oxic environments, the higher the

sedimentation rate the greater the chance that organic matter will be preserved as it is exposed to fewer forms of oxidation and degradation (Peters et al., 2005b). In anoxic environments the amount of organic matter preserved is independent of sedimentation rate. Oxic and anoxic environments themselves are key factors in the preservation of biomarkers. Anoxic conditions enhance preservation of biomarkers and other organically derived matter, while oxic conditions destroy most traces of any organic matter during sedimentation and even diagenesis (Peters et al., 2005b). Many factors contribute to the oxidation of organic matter. The main factors are highly oxidized fluids that flow through the rocks or when oxidized minerals are present, like hematite (Sumner, 2004). This is one reason why the siliciclastic rocks of the Nippewalla Group are not good candidates for biomarker preservation, as the grains in these rocks are coated with hematite. Oxidation of organic matter can also be caused by bioturbation from metazoa, and other organisms, as these benthic organisms actually oxidize the organic material present (Peters et al., 2005b) and severely inhibit their preservation. In anoxic environments bioturbation and other aerobic processes are severely limited or otherwise nonexistent (Peters et al., 2005b) enabling the organic matter preservation.

Different types of biomarkers that can be preserved include hopanes, nor-hopanes, me-hopanes, steranes, *n*-alkanes, pristane, and phytane (Peters et al., 2005b). These biomarkers can be preserved when given the right environmental conditions, and in most cases they can be traced back to a biological precursor molecule because their basic structures remain intact (Killops and Killops, 2005; Peters et al., 2005b). One method of detecting biomarkers is through the use of a Gas Chromatography Mass Spectrometer (GCMS). A GCMS analyzes the extractable organic matter from the rock and/or mineral. Biomarkers break down in unique fragmentation patterns, based on their structure, when they are ionized by an electron beam

which is shown on the MS. Each class of biomarkers also has a characteristic mass to charge ratio ( $m/z$ ) that is produced by the fragmentation process and can aid in their identification, as this ratio is based on the mass of the biomarker and originates from a portion of the molecule structure itself. Hopanes, nor-hopanes, methyl-hopanes, steranes, *n*-alkanes, pristane, phytane, have an  $m/z$  of 191, 177 and 191, 205, 217, respectively, and 85 for *n*-alkanes, pristane, and phytane. They also have certain retention times, based on the size of the molecules, read by the GC. Elution patterns are considered diagnostic, as groups of biomarkers tend to elute in a particular manner, which is based on their molecular weight and volatility (Peters et al., 2005b).

Hopanes are biologically specific, and can be related back to their original precursor, bacterial membranes (Peters et al., 2005a). Typically, hopanes contain 27-35 carbon atoms in their structure and have a  $m/z$  of 191. Hopanes (Figure 1.3) that contain 31 or more carbon atoms, referred to as homohopanes, can indicate bacteriohopanepolyols, which are common in prokaryotic microorganisms, and if they contain 30 or less they are referred to as normal hopanes, and can originate from other pentacyclic triterpenoids like diploptene or diplopterol, mostly indicating higher plants (Killops and Killops, 2005; Peters et al., 2005a; Prah et al., 1992). There are many ratios that can be used in order to better evaluate the depositional environment. These ratios can help identify the source rock of the organic matter, determine if it is marine or lacustrine, or if the source rocks are from carbonate or hypersaline conditions (Peters et al., 2005a). Examples of these ratios are the  $C_{29}/C_{30}$ ,  $C_{31}/C_{30}$ , and the Ts/Tm ratios. The  $C_{29}/C_{30}$  ratio is able to better identify the source rock of the organic matter as  $C_{29}$  represents carbonate or evaporite organic material, the  $C_{31}/C_{30}$  ratio helps determine if the source rock is marine or lacustrine origin, and the Ts/Tm ratio can indicate source rocks from carbonates or hypersaline conditions (Connan et al., 1986; Elfadly et al., 2016; Peters et al., 2005a; Roushdy et

al., 2010). There are two other types of hopanes that are identified in this study, with one being nor-hopanes.

Nor-hopanes (Figure 1.3), specifically 25-nor-hopanes, are structurally similar to hopanes and are the result of heavy biodegradation of hopanes. The origin of nor-hopanes is still speculated by many researchers, however, they are thought to have formed from the demethylation of hopanes and subsequently have similar microbial precursors (Peters and Moldowan, 1991; Peters et al., 2005a). They can be identified using the  $m/z$  of 177 and  $m/z$  of 191. The other type of hopane are the methylhopanes. Methylhopanes (me-hopanes) (Figure 1.3) are hopanes with the addition of a methyl group to the ring A/B fragment (Peters et al., 2005a). This addition increases the diagnostic fragmentation of  $m/z$  191 to  $m/z$  205. They can be a useful correlation tool in the sense that ratios of me-hopanes to hopanes can be used to determine source input that is representative of the bacterial populations at the time of deposition (Peters et al., 2005a). Me-hopanes are of prokaryotic origin and were thought to only originate from cyanobacteria (Farrimond et al., 2004; Welander et al., 2010). However, they are now thought to originate from not only cyanobacteria, but from methanotrophic bacterium, and nitrogen-fixing bacteria as well (Farrimond et al., 2004).

Steranes (Figure 1.4) originate from sterols, which are constituents of membranes and hormones of eukaryotic organisms. They can be identified using the  $m/z$  of 217 (Peters et al., 2005a). Steranes commonly range in chain length from  $C_{26}$  to  $C_{30}$  and can be indicative of multiple environments. For instance,  $C_{29}$  steranes are thought to be associated with terrigenous organic matter, since the  $C_{29}$  sterol precursors are common in vascular plants (Volkman, 1986), while  $C_{30}$  steranes are indicative of marine sources as they are thought to originate from marine invertebrates and marine algae (Moldowan et al., 1985).

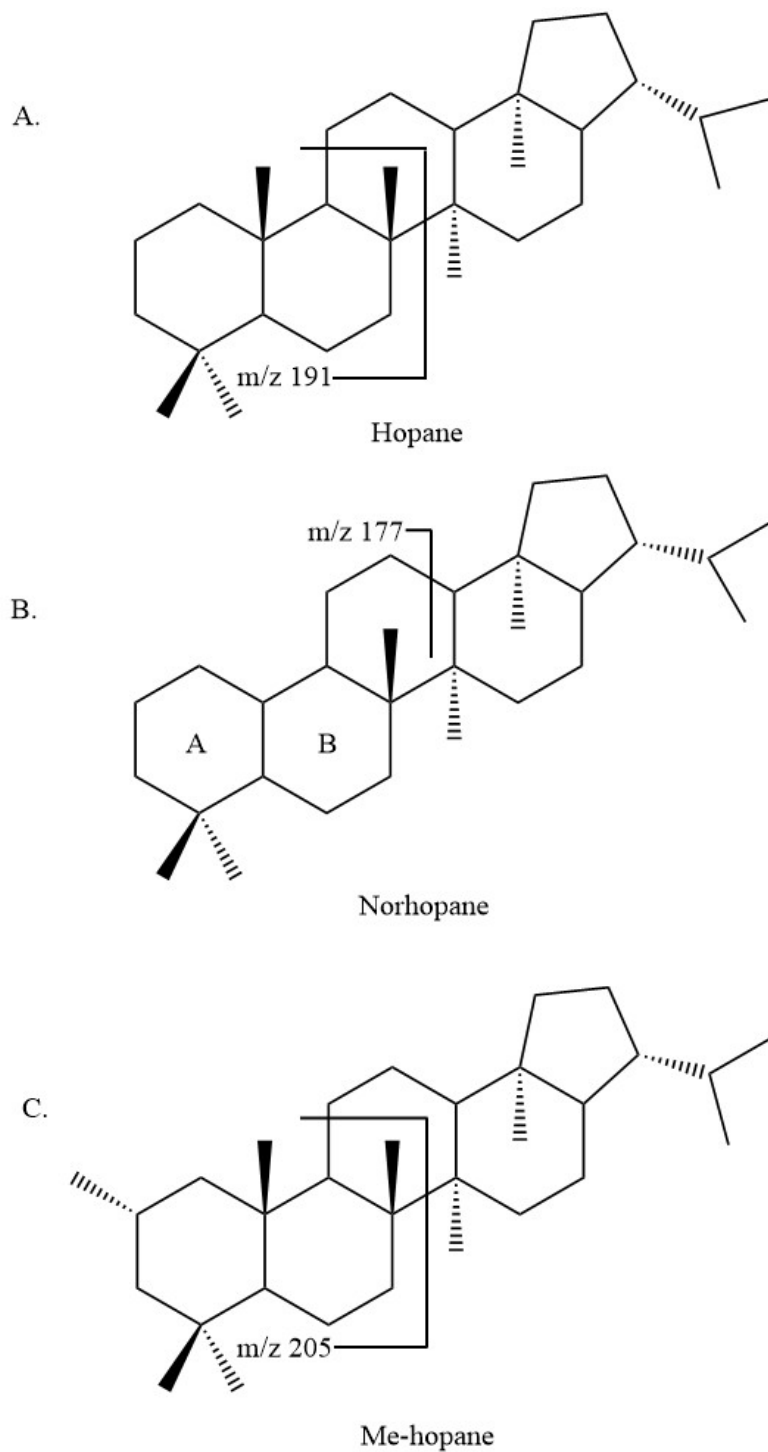


**Figure 1.3:** Structures of hopane molecules referenced for analysis. A - Generalized hopane structure. B - Norhopane structure lacking a methyl group at the A/B fragment. C - Me-hopane with the addition of a methyl group attached to the A cyclohexane ring.

*n*-Alkanes (Figure 1.4) are not biologically specific like the different types of hopanes and steranes, however, they can be used to determine depositional environments, based on ratios of certain *n*-alkanes and their abundancies and patterns created as they elute on chromatograms. For example, a sample with *n*C<sub>17</sub> as its most abundant peak is interpreted to originate from algae in a lacustrine or marine environment (Peters et al., 2005a). They are identified using the *m/z* of 85 and can have a wide range of chain lengths from C<sub>12</sub> to C<sub>35</sub>. Examples of different ratios used in order to determine organic input from different environments are the terrigenous/aquatic ratio (TAR) and the carbon preference index (CPI) (Peters et al., 2005a). The TAR ratio is a function of the summation of *n*-alkanes, C<sub>27</sub>, C<sub>29</sub>, and C<sub>31</sub> divided by the summation of *n*-alkanes C<sub>15</sub>, C<sub>17</sub>, and C<sub>19</sub>  $((nC_{27} + nC_{29} + nC_{31})/(nC_{15} + nC_{17} + nC_{19}))$  (Peters et al., 2005a). The *n*-alkanes C<sub>27</sub>, C<sub>29</sub>, and C<sub>31</sub> are indicative of land-plant organic matter, while the *n*-alkanes C<sub>15</sub>, C<sub>17</sub> and C<sub>19</sub> are indicative of aquatic organic matter, therefore, enabling this ratio to delineate whether there was more terrigenous or aquatic input during deposition (Peters et al., 2005a). The CPI ratio compares the *n*-alkanes C<sub>25</sub> – C<sub>35</sub> with odd carbon number preference to the *n*-alkanes C<sub>24</sub> – C<sub>34</sub> with even carbon number preference (Peters et al., 2005a). Typically, when there is a predominance of odd numbered carbon atoms this indicates input from land-plant organic matter, because these *n*-alkanes typically originate from epicuticular waxes from higher plants, while when there is no predominance or a slight even numbered carbon atoms predominance this can indicate hypersaline carbonate or evaporite sources, based on the fact that these *n*-alkanes are of aquatic origin (Peters et al., 2005a).

Pristane and phytane (Figure 1.4) are thought to originate from the phytol side chain of chlorophyll a, bacteriochlorophyll a and b in purple sulfur bacteria, or from other archaeal membrane components, associating it with phototrophic organisms, and is identified with the *m/z*

of 85 (Peters et al., 2005a; Powell and McKirdy, 1973). Commonly, the pristane/phytane ratio (Pr/Ph) is used to further deduce environments of deposition. When this ratio is less than one it indicates anoxic conditions, greater than one, oxic conditions (Peters et al., 2005a). This is due to the fact that under anoxic conditions phytol is reduced to form phytane and in oxic conditions phytol is oxidized to form pristane. If this ratio is significantly less than one it can indicate hypersaline or carbonate environments due to the presence of less oxygen, or if is greater than three, it can indicate terrigenous organic matter input as it is more exposed to oxic conditions (Peters et al., 2005a; Powell and McKirdy, 1973).

While the presence of biomarkers are an important aspect in determining preservation processes and paleoenvironments, fluid inclusions can play an important role as well. They can often form while the minerals are being precipitated.

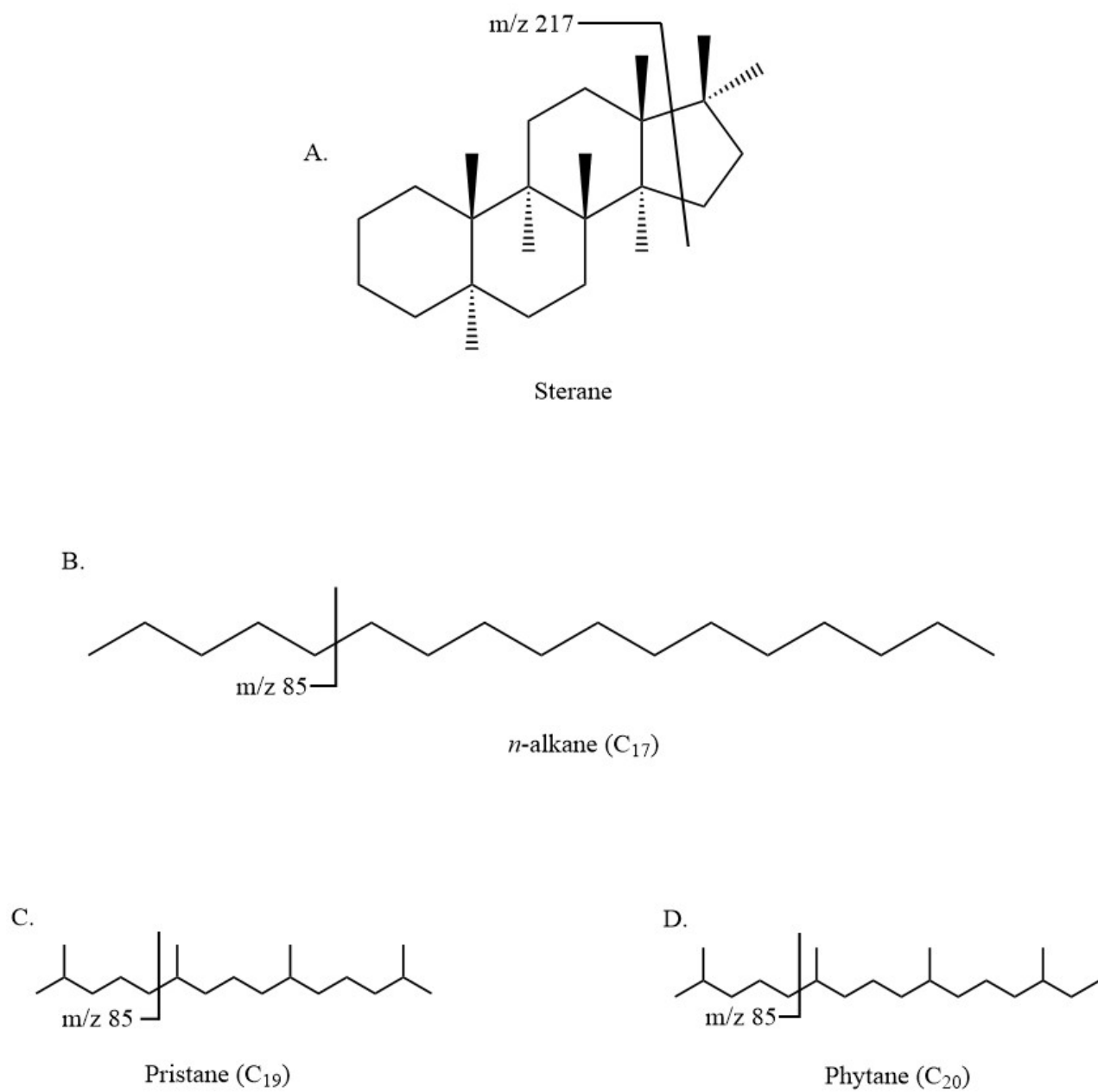


**Figure 1.4:** Molecular structures referenced for analysis. A - Generalized sterane structure. B - Generalized  $n$ -alkane structure; this depicts  $n$ - $C_{17}$ . C - Pristane structure D - Phytane structure.

## 1.4 Fluid Inclusions

Fluid inclusions can provide important paleoenvironmental information as well as petrological details used for interpretation of mineral and rock growth. They can entrap numerous constituents, including different types of algae, prokaryotic cells and other types of microorganisms or organic matter, hydrocarbons, water, brines, gases, and other minerals (Bodnar, 2003; Conner and Benison, 2013; Lowenstein, 2012). As crystals grow in the presence of fluids, or other components, the fluid can be trapped and form fluid inclusions. Fluid inclusions do not always have to contain fluid, and in fact, they can contain, liquid, gas, solids, or a combination of all three (Bodnar, 2003). Three terms are applied to classifying fluid inclusions, primary, secondary, and pseudosecondary (Bodnar, 2003; Goldstein and Reynolds, 1994). Primary fluid inclusions are inclusions that are trapped typically along a growth band, indicating it formed during and as a result of crystal growth. Secondary inclusions are inclusions that are trapped once the crystal is completely formed. They occur when deformation events occur, typically fractures. When these types of features occur, fluid inclusions can form along these fractures. Pseudosecondary fluid inclusions are similar to secondary inclusions in that they also form along fractures in the crystal, however, pseudosecondary inclusions are followed by continued growth of the crystal (Bodnar, 2003; Goldstein and Reynolds, 1994). There is also a fourth term that can be applied to classifying fluid inclusions called indeterminate. This is applied to fluid inclusions of which the origin cannot be determined (Goldstein and Reynolds, 1994). The following studies contain fluid inclusions of mostly primary origin that contain multiple phases, vapor, liquid, or solid.

Benison (2013) conducted studies on modern fluid inclusions in gypsum of recent sediments in Western Australia. This gypsum is precipitating in an acid saline lake environment

similar to what the Nippewalla Group once was. Using a petrographic microscope, Benison (2013) found fluid inclusions that contained one or multiple phases (liquid, vapor, solid). The three phases the inclusions contained were, solid hematite and kaolinite, and fluid from shallow lake water. Unfortunately, no organic matter was found in the gypsum, however, it was discovered in the halite of this area, opening up the possibility of organic matter being preserved in gypsum.

Another modern study at Salars Gorbea and Ignorado, located in northern Chile, by Benison and Karmanocky (2014), looked at fluid inclusions in the gypsum being precipitated there and what was contained within them. The study focused on two types of gypsum, bottom-growth gypsum and reworked grains of gypsum. They found a plethora of microorganisms entrapped in fluid inclusions of both types of gypsum. These included diatoms, suspect green algae and other types of algae, and prokaryotes which were found in both fluid inclusions and entrapped in the gypsum itself.

## CHAPTER TWO: Sample Collection and Methods

### 2.1 Field Site

The Dog Creek, Blaine, and Flowerpot Shale formations of the Nippewalla Group crop out as buttes and mesas near Medicine Lodge, KS located in Barber County (Figure 1.2). This area is formally known as both the Gypsum Hills, because of the vast amounts of gypsum present, and the Red Hills, due to the red staining caused by the hematite. The Blaine Formation caps most the of the buttes and mesas (Figure 2.2) in the area, forming an easily recognizable resistant ledge of gray/blue anhydrite and gypsum (Benison, 1997; Benison et al., 2015). The underlying unit, the Flowerpot Shale, consists of red to gray arenaceous shale, red to gray siltstone, and red fine-grained sandstone (Benison, 1997; Benison et al., 2015). Deposits of gypsum and anhydrite are also contained within the Flowerpot Shale. Lastly, the Dog Creek Formation, which is the youngest rock unit in the Nippewalla Group, is made up of mostly red siltstone, red mudstone, friable, fine-grained, massive bedded red sandstone and thin anhydrite beds and can be seen along road cuts (Benison, 1997).

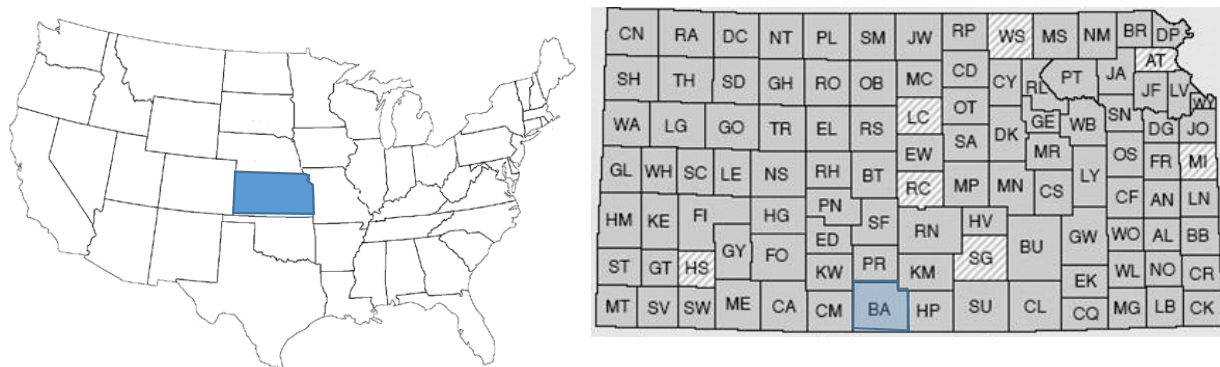


**Figure 2.1:** Map showing the location of Kansas and Barber County.



**Figure 2.2:** Field photo of a butte in Sun City, KS capped by the Blaine Formation overlying the Flowerpot Shale. The Blaine Formation is distinguished by its gray color.

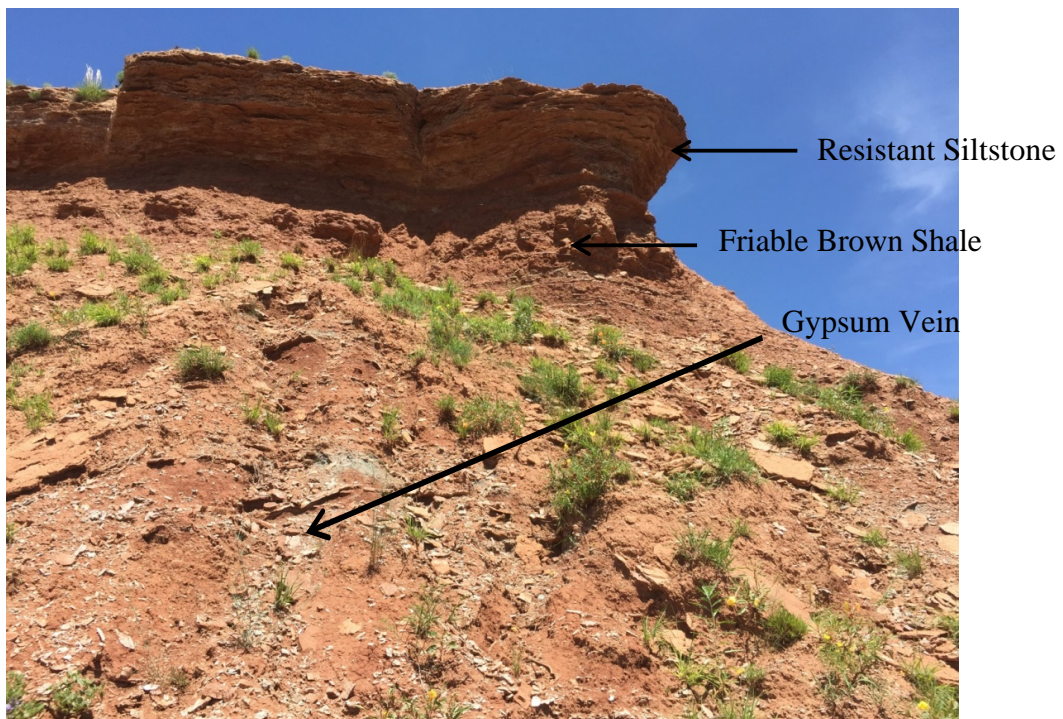


**Figure 2.3:** Field photo of the Flowerpot Shale. Beds of resistant, ledge forming, red to gray siltstone, overlie friable brown to red shale. Veins of gypsum and anhydrite occur locally, but are not as visible in this photo.



**Figure 2.4:** Sandstone beds of the Dog Creek Formation, located approximately 14 miles west of Medicine Lodge, KS, showing the massive red sandstone (middle) and friable sandstone (top).

## 2.2 Sample Collection

A total of 13 samples were collected from outcrops of the Dog Creek, Blaine, and Flowerpot Shale formations in sections that are located near Medicine Lodge, KS and Sun City, KS. Each sample was chosen based on its mineralogy and sedimentology. Beds that contained either entirely gypsum or variant amounts of gypsum were sampled: beds containing no gypsum were targeted for comparison. The samples collected are red fine-grained sandstone and siltstone, and unconsolidated sandstone from the Dog Creek Formation; unconsolidated and consolidated white gypsum, and green/gray gypsum from the Blaine Formation; and red, gray, and brown shale, arenaceous shale, and satin spar from the Flowerpot Shale.

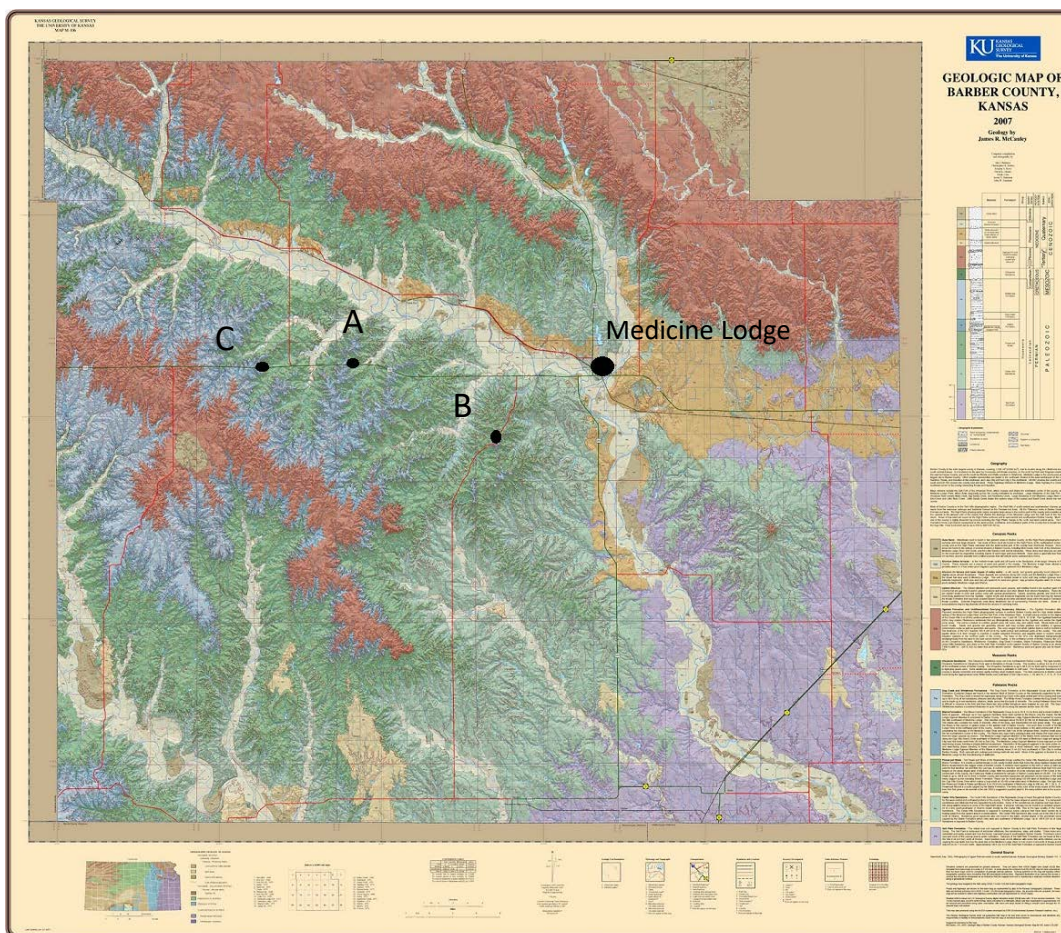


**Figure 2.5:** Map of Barber County showing the locations of the sampling sites near Medicine Lodge, KS. Site A: Flowerpot Shale (37° 16' 58.01" N 98° 46' 17.04" W); Site B: Blaine Formation and Flowerpot Shale (37° 14' 36.95" N 98° 39' 49.88" W); Site C: Dog Creek Formation (37° 16' 50.94" N 98° 50' 51.11" W). ([http://www.kgs.ku.edu/General/Geology/County/abc/ba/gifs/M106\\_BarberGeology\\_042307 .pdf](http://www.kgs.ku.edu/General/Geology/County/abc/ba/gifs/M106_BarberGeology_042307.pdf))

### 2.3 Sample Preparation

All glassware, including different sizes of beakers, funnel tops and funnel stems (for filtering), Erlenmeyer filter flasks, 7.62 cm and 10.16 cm glass tubes, and GC vials were combusted overnight at 450 °C to remove any contaminants. Any glassware or other type of container or tool used was solvent rinsed with methanol (MeOH), dichloromethane (DCM) and hexane to prevent any contamination from occurring during the analysis process.

Each rock or mineral sample was placed in a 250 mL beaker, which was filled with dichloromethane (DCM) until covered, and placed in an ultrasonicator bath for approximately 5 minutes at 24 °C. This process helps to eliminate any contaminants that may be present on the rock samples themselves. The samples were set out to dry, for approximately 10 minutes, and were then crushed and powdered using a Retsch Ballmill that was washed with soap and water, and then solvent rinsed with all three solvents. The Retsch Ballmill powdered the samples at 280 rpm at 5 minute intervals until the sample was completely powdered to obtain 300 g for analysis.

### **2.3.1 Solvent Extraction**

Once the samples were powdered, 300 g of sample were placed in 12 Teflon tubes, 25 g in each tube, in preparation for solvent extraction using a MARS Xpress microwave-assisted solvent extraction system. Then, a mixture of 22.5 mL of DCM and 2.5 mL of MeOH, a 9:1 ratio, is placed in each tube along with the 25 g of sample. After this has occurred the tubes are placed in the MARS Xpress microwave at 100 °C, 800 W, and a 40 minute extraction time to remove all of the extractable organic material. Once the extraction process is complete, each sample is vacuum filtered into a filtering flask.

The next step in the process is to evaporate and condense the extracted solvent to dryness and bring it back up in approximately 200 µL of hexane. After the filtration, a glass pipette is used to pipette and distribute the solvent into six 10.16 cm glass tubes. These glass tubes are then placed in a TurboVap, which contains a bath of deionized water and blows a steady stream of nitrogen gas onto the samples. The TurboVap is run for 10 minute intervals at 30 °C until enough solvent is evaporated to fit into a 1.5 mL glass vial. To ensure no solvent is left behind, during the transferring process, two rinses of DCM and one rinse of hexane is used in each 4”

glass tube. Once the extract is able to fit into the 1.5 mL glass vial it is blown down to dryness and brought back up in approximately 200  $\mu$ L of hexane. The 200  $\mu$ L are then transferred to a GC vial using a glass syringe. Concentrating the sample is important before it is placed in the Gas Chromatography Mass Spectrometer (GCMS); 300 g of highly concentrated sample must be available for analysis in order to give off a detectable amount of signal to accurately analyze the data. Once the sample is transferred to a GC vial it is ready to be analyzed with the GCMS.

### **2.3.2 GCMS Analysis**

The concentrated sample is analyzed by a ThermoFinnigan Trace GC-DSQ quadrupole mass spectrometer using full scan mode beginning at 40  $^{\circ}$ C with a 20  $^{\circ}$ C per minute increase to 130  $^{\circ}$ C followed by a 5  $^{\circ}$ C temperature increase up to 350  $^{\circ}$ C maximum. During this time the concentrated sample was separated by gas chromatography and then the separated compounds were transferred to the mass spectrometer.

The GCMS detects the molecules that are present in the sample representing them as peaks in the gas chromatogram. Larger molecules elute later in the chromatogram and shorter molecules elute earlier. A molecules' mass spectrum is a characteristic pattern of how the molecules fragment during the ionization process, which is when the eluted compounds pass into the ionizing chamber of the mass spectrometer and are ionized by an electron beam. This renders the molecules identifiable as they pass through the mass analyzer and into the electron multiplier (Peters et al., 2005). Using a Mass Spectrum library database created by the National Institute of Standards and Technology (NIST), the mass of the molecular fragments displayed by the mass spectrometer data, and other literature, the molecules present in the samples were identified.

Two methods were used while running the GCMS. One method analyzed the full spectrum of possible biomarkers in a given sample and was originally used. Most samples were noisy, however, so the Selective Ion Monitoring (SIM) method was adopted. This method scanned the sample for selected ions that were input prior to being analyzed. Ion masses selected to be analyzed were 85, 113, 131, 191, 205, and 217, which would indicate possible, *n*-alkanes, isoprenoids, carotenoids, hopanes, me-hopanes, and steranes, respectively.

## **2.4 Analysis of TOC**

The Total Organic Carbon (TOC) is a quantitative analysis of the organic carbon contained within a given sample. This measurement is typically used to determine if a formation is capable of generating and storing hydrocarbons and, therefore, worth drilling (Jarvie, 1991). For this study the TOC was determined to better understand the total volume of organic matter present in each sample when used in conjunction with the GCMS data.

The samples were powdered using the Retsch Ballmill for 5-10 minutes at 280 rpm to obtain approximately 5 g of sample. Once this was obtained the powdered 5 g of sample for each rock were placed in 50 mL centrifuge tubes. After this step, 30 mL of 0.5M HCl was placed in each 50 mL tubes, which were shaken vigorously to dissolve any inorganic carbon present in the sample and then placed in a centrifuge at 4000 rpm for two minutes. The acid was then decanted and replaced, and the shaking and centrifuging was repeated, until there was no longer a reaction with inorganic carbon. All samples were then rinsed with nanopure water until they obtained a pH of 6 or 7. After they were neutralized the samples were freeze dried using liquid nitrogen and then placed in a Labconco Freezone 4.5 Model 77500 freeze dryer and dried over night at -52 °C with a vacuum of  $45 \times 10^{-3}$  mbar.

After freeze drying, 5 mg to 30 mg of sample (depending on rock type) was weighed out into 5x9 mm pressed tin capsules. These were then combusted at 980 °C in a Costech Instrument Elemental Combustion System (ECS) 4010 where the resultant gas was transferred to a Thermo Finnigan MAT 253 Stable Isotope Mass Spectrometer, in continuous flow mode, via a Thermo Finnigan Conflo III (Brenna et al., 1997). The resultant data was recorded as C% (TOC).

## **2.5 Thin Section Analysis**

From the samples that were collected in the field 13 thin sections were made in the KU thin section preparation laboratory. Of these, 11 were impregnated with epoxy. Two of the 13 samples were made into thick sections for fluid inclusion analysis and were impregnated with super glue rather than epoxy. Two Olympus BX51 petrographic microscopes were used for the analysis. One was equipped with reflective light and transmitted light microscopy with 10x (N.A. = 0.30), 20x (N.A. = 0.45), 50x (N.A. = 0.80), and 100x (N.A. = 1.30) oil immersion objectives and a digital camera. The other contained two exciter filters designed to transmit a UV wavelength of 330 – 385 nm and a violet-blue wavelength of 400 – 440 nm. This microscope was equipped with 4x (N.A. = 0.13), 10x (N.A. = 0.30), 20x (N.A. = 0.45), and 50x (N.A. = 0.8) objectives and a digital camera.

## CHAPTER THREE: Results

### 3.1 Organic Matter Content

It is important to note that the rock and mineral samples collected for biomarker analysis were very organically lean. A typical biomarker analysis following the methods outlined in chapter 2 requires 3 g – 5 g of rock per sample, but to obtain reliable results in this study, 300 g of rock per sample was needed from the Nippewalla Group. Consequently, there were low concentrations of biomarkers in the samples that yielded interpretable data. Due to the organic-lean nature of the rocks and minerals analyzed the chromatograms often had a low signal to noise ratio, making identification and interpretation difficult. To counteract this issue all samples were ran through the GCMS again using a Selected Ion Monitoring (SIM) method described previously in the methods section.

### 3.2 Co-elution

Due to the co-elution of certain *n*-alkanes in the samples it was difficult to ascertain their exact elution time. Unfortunately, this renders some of the ratios inaccurate, specifically for the Pr/Ph ratio and the Pr/*n*C<sub>17</sub> ratio. Often, Pr and *n*C<sub>17</sub> co-elute making the identification and separation of these two compounds difficult. This was the case for the GG#1 sample (Table 3.1) and is shown by an asterisk in the chromatogram (Figure 3.4). All other ratios were measured as accurately as possible given the data from the organically – lean samples.

### 3.3 Biomarker Analysis

#### 3.3.1 Hopanes

Of the 13 samples collected, only three samples contained hopanes and variants of hopanes (Figure 3.1). These samples were collected from the unconsolidated and consolidated white gypsum (CG#1) and the green/gray gypsum (GG#1) of the Blaine Formation and from shale containing gypsum and anhydrite from the Flowerpot Shale Formation (FSG#1) (Table 3.1). There were no hopanes identified in samples collected from the Dog Creek Formation. CG#1 (unconsolidated and consolidated white gypsum) contained homohopanes, C<sub>31</sub> – C<sub>35</sub>, and normal hopanes, C<sub>29</sub> and C<sub>30</sub>, with the C<sub>35</sub> homohopane being the most abundant. There was also a 25-norhopane C<sub>30</sub>, trisnorneohopane Ts, and the trisnorhopane Tm, in the white gypsum of sample CG#1. Sample GG#1 (green/gray gypsum) contained a series of me-hopanes, C<sub>31</sub> – C<sub>33</sub>, with the C<sub>31</sub> chain length being the most abundant. Samples FSG#1 (Flowerpot Shale sample) contained Ts, Tm, normal hopanes C<sub>29</sub> – C<sub>30</sub>, homohopane C<sub>31</sub>, and 25-norhopane C<sub>30</sub>.

Of the hopanes detected ratios C<sub>29</sub>/C<sub>30</sub>, C<sub>31</sub>/C<sub>30</sub>, and Ts/Tm can be calculated. These ratios were only able to be calculated for the CG#1 sample (Blaine Formation) and the FSG#1 sample (Flowerpot Shale). The C<sub>29</sub>/C<sub>30</sub>, C<sub>31</sub>/C<sub>30</sub>, and Ts/Tm values for CG#1 and FSG#1 are 1.27, 1.01, 0.53 and 0.83, 0.48, 1.03 (Table 3.2) respectively. From the C<sub>29</sub>/C<sub>30</sub> ratio one is able to better identify the source rock of the organic matter. Ratios > 1 are characteristic of carbonates and evaporites (Connan et al., 1986; Roushdy et al., 2010). Values > 0.25 indicate marine source rocks and values < 0.25 indicate lacustrine source rocks for the C<sub>31</sub>/C<sub>30</sub> ratio (Peters et al., 2005). Low Ts/Tm values (< 0.50) can indicate source rocks from carbonates, and high values (> 0.50) can indicate hypersaline conditions (Elfadly et al., 2016; Roushdy et al., 2010). This is due to the fact that Ts is more abundant in oxic or hypersaline conditions, while Tm is more abundant in carbonate settings. Also, this ratio is sensitive to clay-catalyzed reactions, which would indicate a higher ratio in shales and a lower ratio in a carbonate setting (Peters et al., 2005).

<b>Formation</b>	<b>Sample</b>	<b>Description</b>
<b>Dog Creek</b>	DCSS#1	Hematite stained sandstone with minor gypsum
	DC#2	Gray to orange sandstone
	DC#3	Red to brown sandstone
<b>Blaine</b>	CG#1	Unconsolidated/consolidated white gypsum
	GG#1	Green/gray gypsum
<b>Flowerpot Shale</b>	FSG#1	Shale with gypsum
	SP#1	Satin spar, secondary gypsum
	FPA#1	Arenaceous shale
	FP#1	Brown friable shale

**Table 3.1:** Sample identification with lithologic description.

<b>Sample</b>	<b>C<sub>29</sub>/C<sub>30</sub></b>	<b>C<sub>31</sub>/C<sub>30</sub></b>	<b>Ts/Tm</b>
CG#1	1.27	1.01	0.53
GG#1	ND	ND	ND
FSG#1	0.83	0.48	1.03

**Table 3.2:** Calculated ratio values from the hopane samples CG#1, GG#1 and FSG#1.

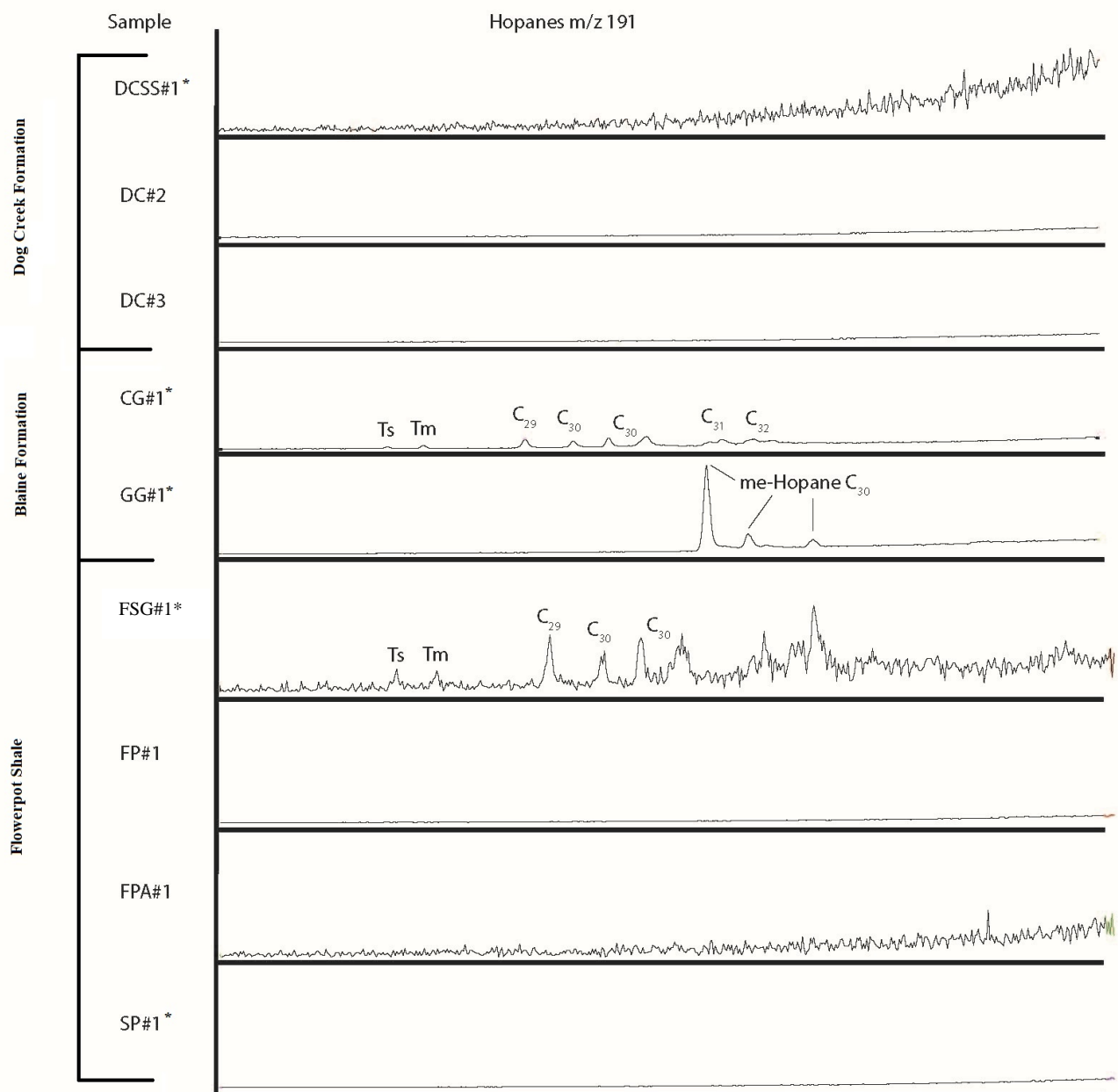


**Figure 3.1:** Chromatograms of hopanes for each rock formation of this study in stratigraphic order starting with the youngest, Dog Creek Formation (DCSS#1, DC#2, DC#3); Blaine Formation (CG#1, GG#1); Flowerpot Shale (FSG#1, FP#1, FPA#1, SP#1). Samples with hopanes are CG#1, GG#1, and FSG#1. CG#1 displays hopanes C<sub>29</sub> – C<sub>32</sub>, along with Ts and Tm, and one nor-hopane, C<sub>30</sub>, that elutes before the C<sub>30</sub> regular hopane. GG#1 shows the me-hopane C<sub>30</sub> that is better displayed in figure 3.2. FSG#1 displays hopanes C<sub>29</sub> – C<sub>30</sub> and also Ts and Tm. Scaled relative to the GG#1 sample. Samples with an asterisk (\*) contain gypsum.

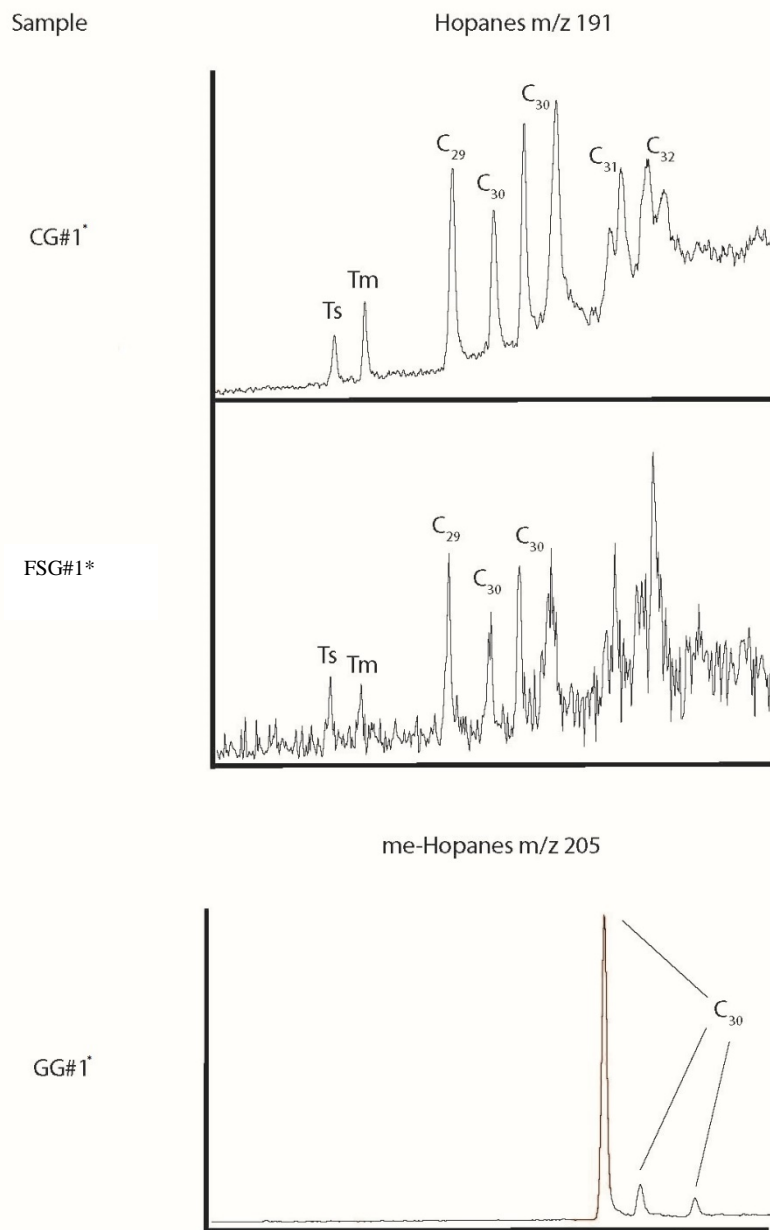


**Figure 3.2:** A better representation of hopanes found in samples CG#1 and GG#1 of the Blaine Formation, and sample FSG#1 of the Flowerpot Shale. CG#1 shows regular hopanes C<sub>29</sub> and C<sub>30</sub>, and homo-hopanes C<sub>31</sub> and C<sub>32</sub>, along with Ts and Tm, which are trisnorneohopanes and trisnorhopanes, respectively. It also shows the nor-hopane C<sub>30</sub> eluting before the regular hopane C<sub>30</sub>. FSG#1 shows all of the same hopanes as CG#1 except it does not contain the homo-hopanes C<sub>31</sub> and C<sub>32</sub>. GG#1 shows the me-hopane C<sub>30</sub>. Scaled relative to the GG#1 sample. Samples with an asterisk (\*) contain gypsum.

### 3.3.2 *n*-Alkanes

*n*-Alkanes of the Nippewalla group were slightly more abundant than the hopanes, and were detected in four out of the 13 samples collected (Figure 3.3 – 3.5). The *n*-alkanes and isoprenoids detected in these samples can be used to calculate a series of ratios to better understand the source rock of these biomarkers and the type of paleoenvironment their biological precursor once inhabited. These include the odd-over-even predominance ratio (OEP), Pr/Ph, ratio, Pr/*n*C<sub>17</sub>, and Ph/*n*C<sub>18</sub> ratios. The OEP ratio was calculated using the *n*-alkanes *n*C<sub>21</sub> – *n*C<sub>27</sub> odd, and *n*C<sub>22</sub> – *n*C<sub>28</sub> even, as these were present in all samples where ratios were calculated. OEP ratio values > 1 (odd-predominance) are interpreted to indicate biomarkers dominated by land-plant organic matter and values < 1 (even-predominance) signifies a marine source, while a slight even-predominance signifies hypersaline carbonate and evaporite source rocks (Elfadly et al., 2016; Peters et al., 2005). A Pr/Ph ratio value > 1 indicates oxic conditions, < 1 indicates anoxic conditions, > 3 indicates terrigenous organic matter under oxic conditions, and < 0.8 can be indicative of anoxic hypersaline or carbonate environments (Didyk et al., 1978; Onojake et al., 2015; Peters et al., 2005; Roushdy et al., 2010). The Pr/*n*-C<sub>17</sub> and Ph/*n*-C<sub>18</sub> ratios can be related to the type of kerogen present at deposition, which in turn can be related to the type of paleoenvironment. To better represent these two ratios, they can be plotted on a Pr/*n*-C<sub>17</sub> vs. Ph/*n*-C<sub>18</sub> log – log cross-plot. This cross-plot represents the type of kerogen (I, II, or III) the biomarkers originated from, oxidizing and reducing conditions, and maturation and biodegradation amounts.

The Dog Creek Formation (Figure 3.3) sample DCSS#1 (Table 3.1), a fine grained, well rounded, well sorted, hematite stained sandstone, contained mostly shorter chained *n*-alkanes ( $\leq nC_{19}$ ). This sample may contain higher chained *n*-alkanes ( $\geq nC_{20}$ ), however this section of the

chromatogram was very noisy making it difficult to ascertain the *n*-alkanes. The chromatograms most likely have biomarkers co-eluting at the most prominent peaks (except for the *n*C<sub>17</sub> peak), making it difficult to decipher the proper biomarker at those peaks. Combining all of these factors the DCSS#1 sample does contain *n*C<sub>17</sub> and a possibility of containing Pr, Ph, *n*C<sub>18</sub> – *n*C<sub>26</sub>. It has a unimodal distribution with *n*C<sub>17</sub> being the most abundant. Unfortunately, no ratios were calculated with this sample due to the unreliability of the noisy chromatogram. Other samples ran from the Dog Creek Formation were the DC#2 and DC#3 samples (Table 3.1). DC#2 was a gray to orange, fine-grained, well rounded, and well sorted sandstone and DC#3 was a red to brown sandstone that was also fine-grained, well rounded and well sorted. Both of these samples were devoid of biomarkers.

The Blaine Formation samples (Figure 3.4), CG#1 and GG#1, both contained short-chained and long-chained *n*-alkanes, *n*C<sub>17</sub> – *n*C<sub>28</sub>. They also contain the isoprenoids Pr and Ph. The CG#1 and GG#1 samples both have bimodal distributions with *n*C<sub>25</sub> and *n*C<sub>17</sub> being the most abundant, respectively. Values for the ratios calculated for the CG#1 sample is 1.19, 0.27, 0.36, and 1.33, representing the OEP, Pr/Ph, Pr/*n*C<sub>17</sub>, and Ph/*n*C<sub>18</sub> ratios. The values for the GG#1 sample are 1.49, 6.71, 0.43 and 0.36 (Table 3.3).

The Flowerpot Shale Formation (Figure 3.5) had one sample that contained *n*-alkanes, which is the FSG#1 sample previously mentioned and another that contained a series of possible short chained *n*-alkanes, which is the satin spar sample (SP#1), a secondary gypsum. The biomarkers in this sample were of too low concentration and the chromatogram was too noisy in order to make an interpretation of the results. Other samples that were devoid of biomarkers were the arenaceous shale (FPA#1) and a brown friable shale (FP#1) (Table 3.1). The FPA#1 sample had only peaks of contaminants. The *n*-alkanes identified in the sample FSG#1 are *n*C<sub>17</sub> – *n*C<sub>27</sub>

and the isoprenoids Pr and Ph. There is a bimodal trend with the distribution of the *n*-alkanes and *n*C<sub>17</sub> is the most abundant. All of the previously mentioned *n*-alkane ratios were able to be calculated for this sample, except for the OEP ratio, and they are 4.33, 0.46, and 0.14 for the Pr/Ph, Pr/*n*C<sub>17</sub>, and Ph/*n*C<sub>18</sub> ratios, respectively (Table 3.3).

Sample	OEP	Pr/Ph	Pr/ <i>n</i> -C <sub>17</sub>	Ph/ <i>n</i> -C <sub>18</sub>
Dog Creek Fm.	ND	ND	ND	ND
CG#1	1.19	0.27	0.36	1.33
GG#1	1.49	6.71	0.43	0.36
SP#1	ND	ND	ND	ND
FP#1	ND	ND	ND	ND
FSG#1	0.95	4.33	0.46	0.14

**Table 3.3:** Ratios values from the *n*-alkanes samples calculated.

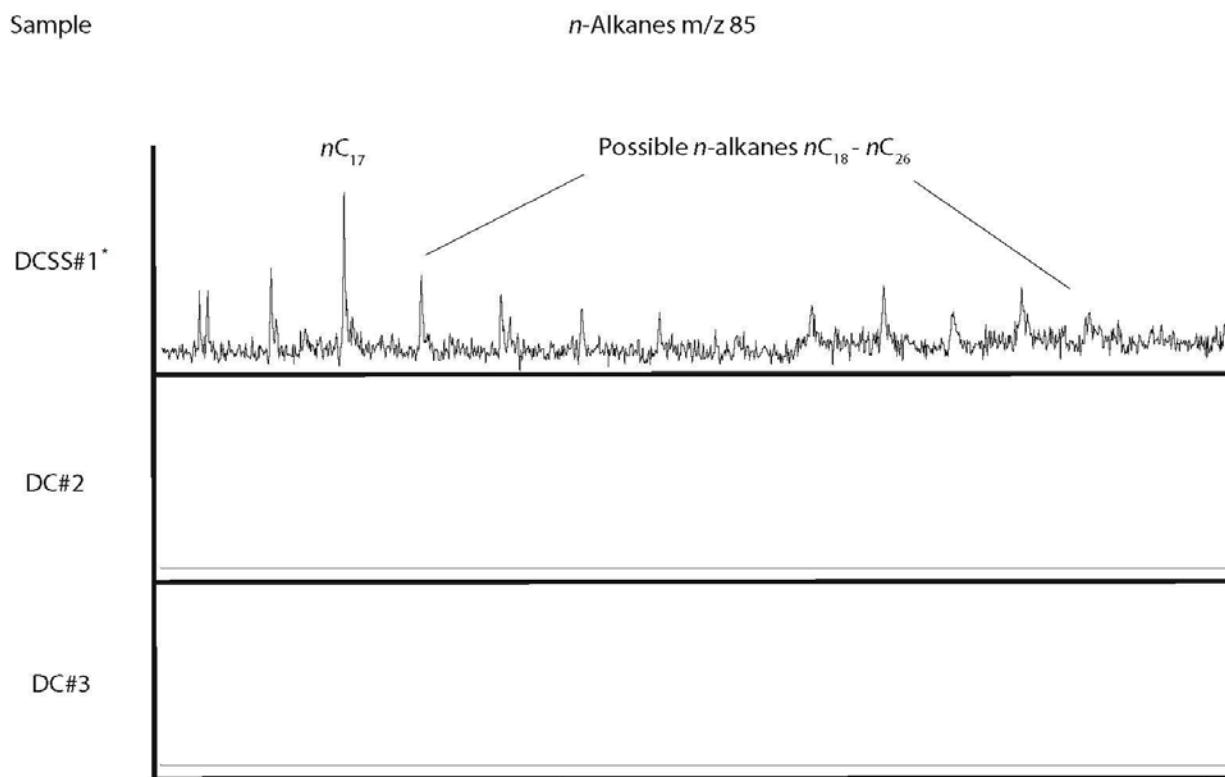


**Figure 3.3:** Chromatograms of samples DCSS#1, DC#2, and DC#3 of the Dog Creek Formation displaying the *n*-alkanes present. DCSS#1 displays *n*C<sub>17</sub> and possible longer chained *n*-alkanes. Samples DC#2 and DC#3 lack any *n*-alkanes or isoprenoids. Scaled relative to the DCSS#1 sample. Samples with an asterisk (\*) contain gypsum.

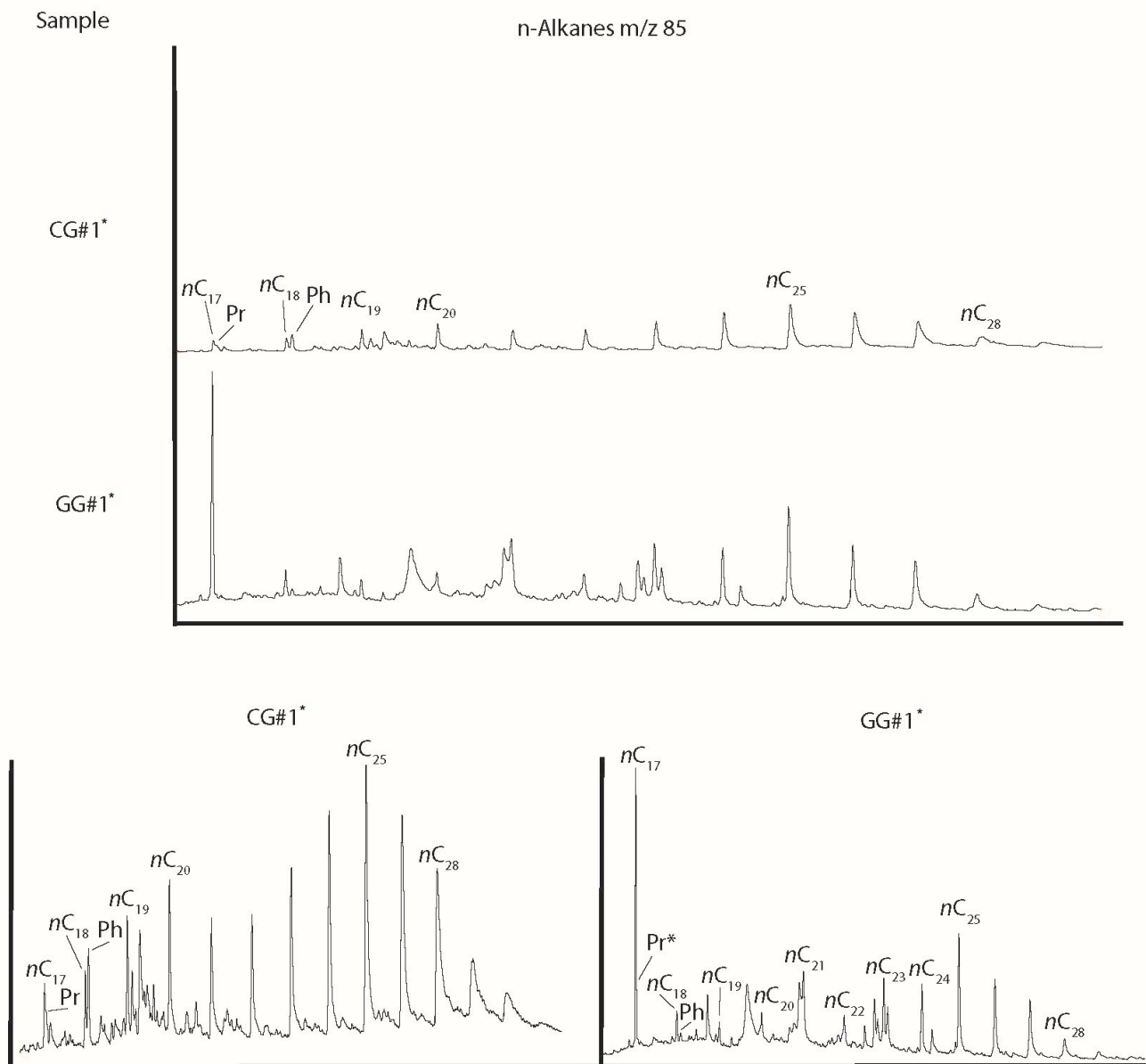


**Figure 3.4:** Chromatograms of samples CG#1 and GG#1 from the Blaine Formation. Top: stacked chromatograms show *n*-alkanes *n*C<sub>17</sub> – *n*C<sub>28</sub>, along with the isoprenoids Pr and Ph. Scaled to the GG#1 sample. Bottom Left: sample CG#1 better representing the *n*-alkanes and isoprenoids present. Bottom Right: sample GG#1 displays a better representation of the *n*-alkanes and isoprenoids present. In this chromatogram Pr is marked by an asterisk (\*) as it is co-eluting with *n*C<sub>17</sub>. Bottom two chromatograms are scaled to themselves. Samples with an asterisk (\*) contain gypsum.

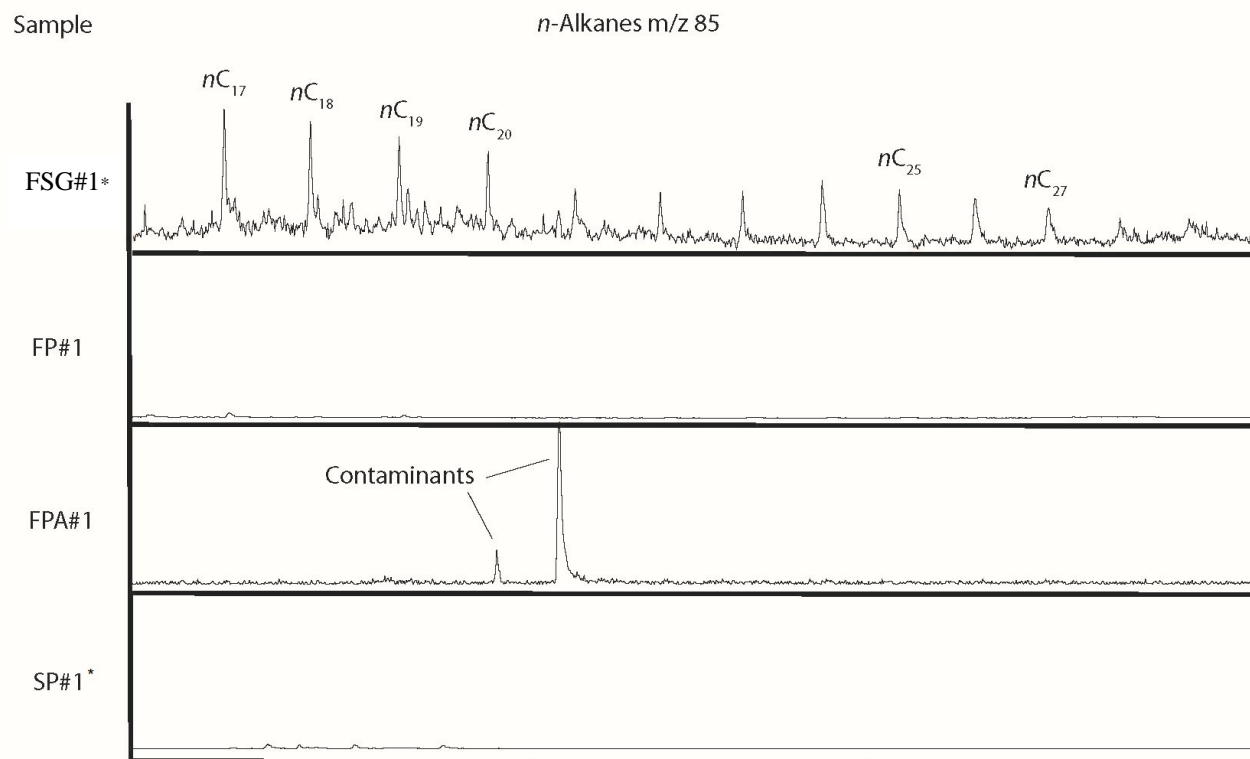


**Figure 3.5:** Chromatograms of samples FSG#1, FP#1, FPA#1, and SP#1 of the Flowerpot Shale displaying *n*-alkanes present. FPG#1 shows the isoprenoids Pr and Ph, and *n*-alkanes  $nC_{17} - nC_{27}$ . FP#1 and SP#1 show no *n*-alkanes. FPA#1 display only contaminants. Scaled relative to the FPG#1 sample. Samples with an asterisk (\*) contain gypsum.

### 3.4 TOC Analysis

As mentioned above, the TOC content (Table 3.4) of each sample was extremely low, indicating the fact that these rocks and minerals are very organically lean. They ranged from 0.01% to 0.08% throughout each formation (Table 3.4). The sample with the highest TOC content of 0.08% was sample FP#1, which is brown friable shale from the Flowerpot Shale Formation. The samples with the lowest TOC content was the CG#2 and the SP#1 from the Blaine Formation and the Flowerpot Shale, respectively, both having 0.01%.

Sample	TOC (%)
DCSS#1	0.03
DC#2	0.02
DC#3	0.03
CG#1	0.02
CG#2	0.01
GG#1	0.02
GG#2	0.04
FP#1	0.08
FP#2	0.07
FPA#1	0.05
FSG#1	0.05
SP#1	0.01
SP#2	0.02

**Table 3.4:** TOC percentages for each sample.

### 3.5 Thin Section Analysis

Thin sections were made of each different rock type and mineral collected from the field. The Dog Creek Sandstone samples were composed of mainly hematite and quartz grains. The Flowerpot Shale samples contained hematite crystals, quartz grains, and minor amounts of gypsum (depending on the sample) (Figure 3.6). Thin sections from the Blaine Formation (CG#1

sample) contained primary gypsum along with a number of fluid inclusions that are of primary origin and mostly a single liquid phase. The GG#1 sample also contained fluid inclusions that were of secondary and pseudosecondary origin, and mostly single phase, however, at least one inclusion had two phases, liquid and gas. In this sample glauconite and was minor amounts of hematite were identified. Small amounts of glauconite in the CG#1 sample were identified as well (Figure 3.7).

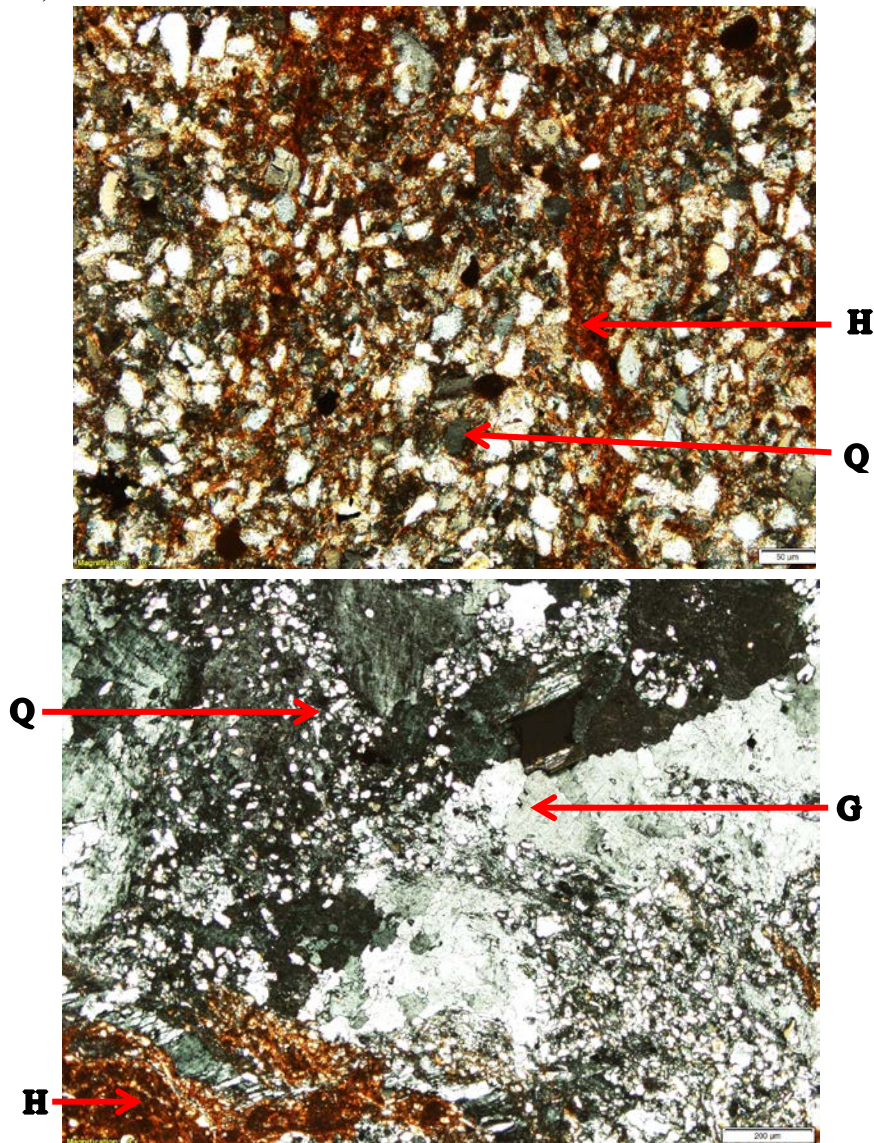


**Figure 3.6:** Top: Dog Creek Formation thin section. Shows hematite (H) staining and cement, along with small quartz (Q) grains, and minor amounts of gypsum (G) indicated by arrows. Scale is 50  $\mu\text{m}$ . Bottom: Flowerpot Shale Formation thin section. Shows hematite staining and cement, with large amounts of gypsum and minor amounts of quartz indicated by arrows. Scale is 200  $\mu\text{m}$ . Both are in crossed-nicols.

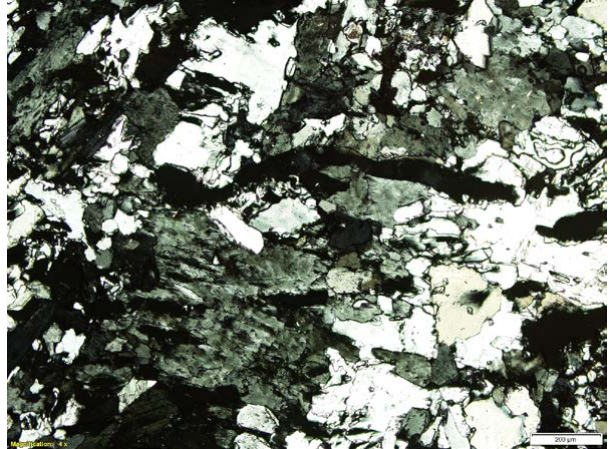
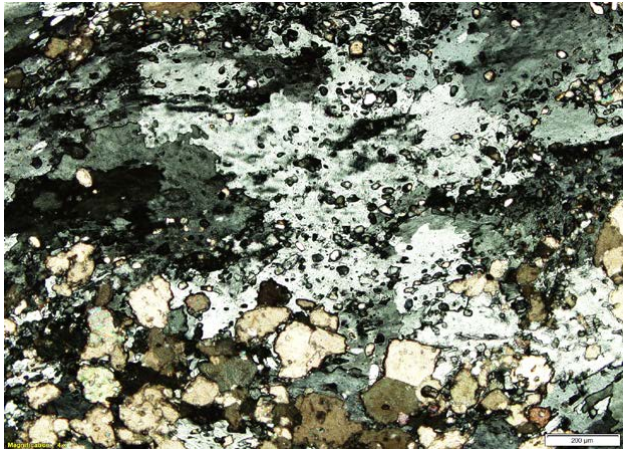
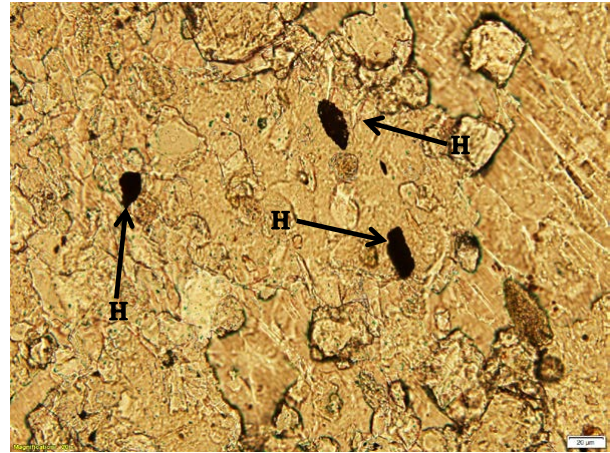
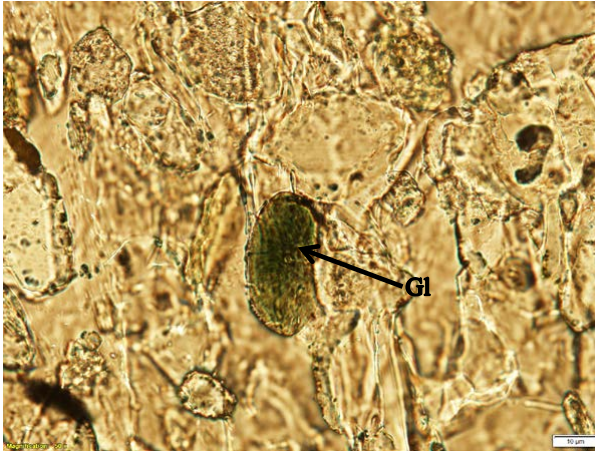


**Figure 3.7:** Top Left: GG#1 sample showing glauconite in transmitted light, scale is 10 µm. Top Right: GG#1 sample showing hematite grains in transmitted light, scale is 20 µm. Bottom Left: GG#1 sample showing gypsum in crossed-nicols, scale is 200 µm. Bottom Right: CG#1 sample showing gypsum in crossed-nicols, scale is 200 µm.

The CG#1 sample (Figure 3.8) show rows of fluid inclusions that look to have grown in the direction of crystal growth. These were not introduced by a fracture in the mineral, indicating primary origin. Even though most of these fluid inclusions did not fluoresce, there were three small fluid inclusions that did, indicating there could be a minute source of organic matter contained within them (Figure 3.8). Evidence of these fluid inclusions being possible sources are indicated by their primary origin and the very small percentage of organic matter that was detected in these sample. It is possible that these fluid inclusions contain a minuscule amount of organic matter, affectively rendering the fluorescence difficult to detect.

Fluid inclusions of the GG#1 sample are mostly of secondary and pseudosecondary origin, although some are of primary origin (Figure 3.9). This interpretation is due to the fact that many of the fluid inclusions were randomly distributed throughout the sample and only one or two existed in a single crystal indicating no direction of crystal growth. The fluid inclusions were of a single liquid phase except for one that contained a gas and liquid phase. This particular fluid inclusion was interpreted as primary as it indicates a growth direction. Unfortunately, because most of the inclusions are not primary it is difficult to ascertain when they actually formed and, therefore, cannot be used to identify an origin of organic matter preserved.

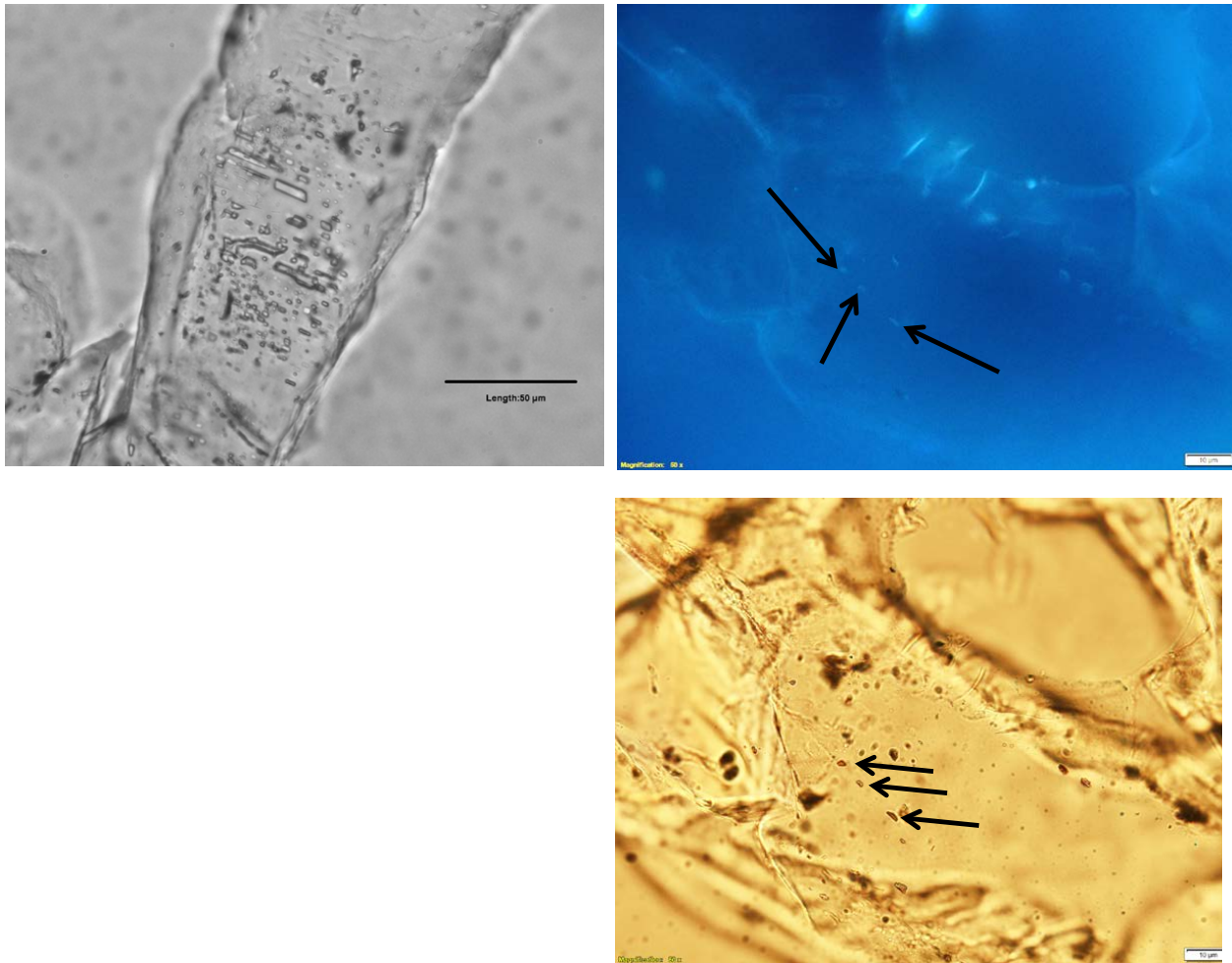


**Figure 3.8:** Photos of fluid inclusions from CG#1 sample. Top Left: Shows rows of fluid inclusions in transmitted light, scale is 50 µm. Top Right: Shows three fluid inclusions that are slightly fluorescing under the blue-violet filter, scale is 10 µm. Bottom Right: Shows the same three fluid inclusions from the top right, only in transmitted light, scale is 10 µm.

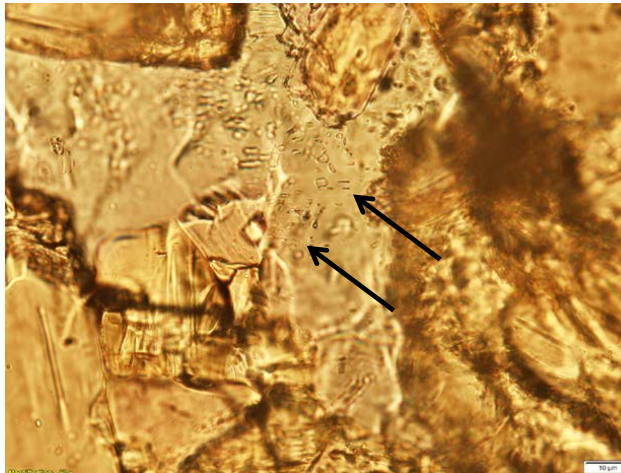
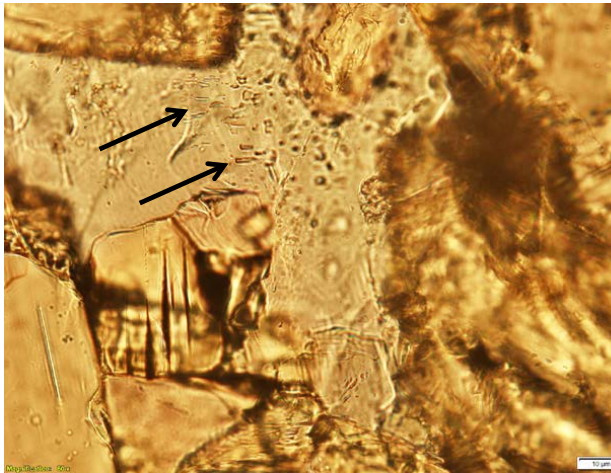
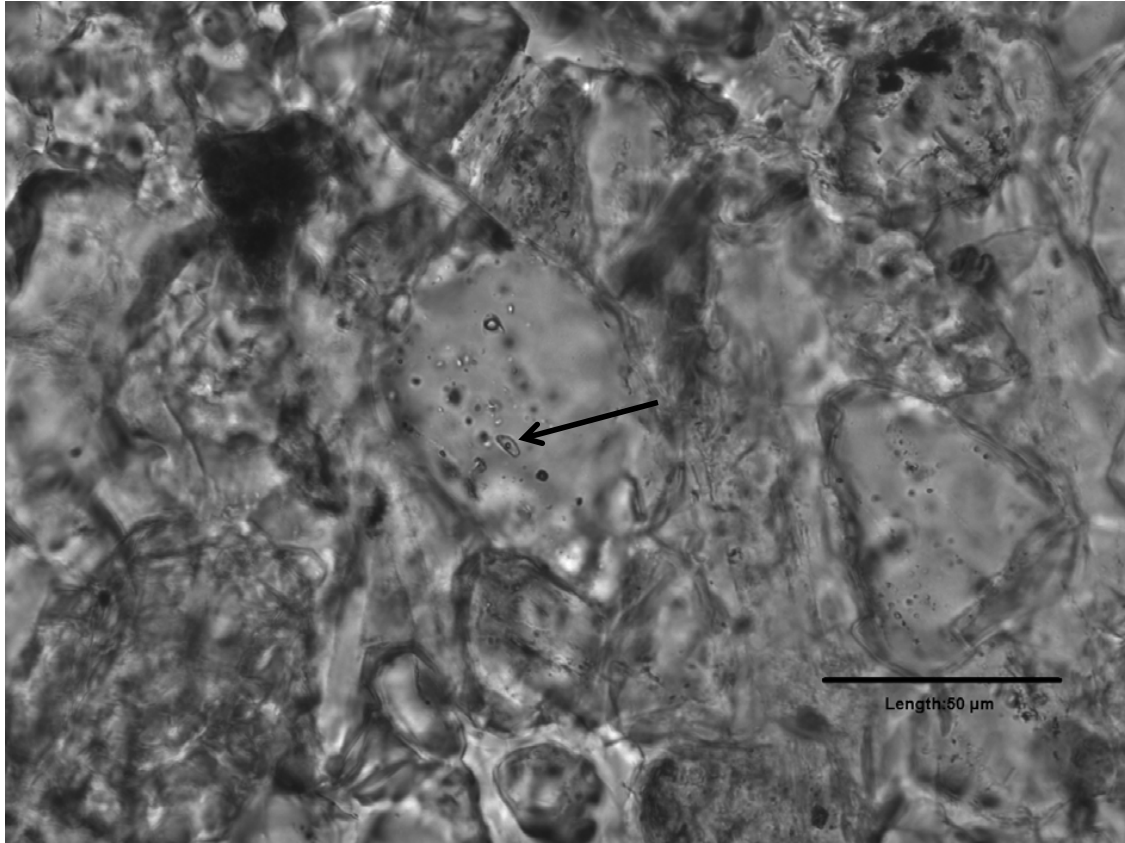


**Figure 3.9:** Photos of GG#1 sample. Top Photo: Shows the two-phase fluid inclusion in transmitted light, scale is 50  $\mu\text{m}$ . Bottom Left: Arrows point to two areas of fluid inclusions, scale is 10  $\mu\text{m}$ . Bottom Right: Arrows point to two areas of fluid inclusions, scale is 10  $\mu\text{m}$ .

## CHAPTER FOUR: Discussion

### 4.1 Modern Contaminants

It is important to be able to distinguish between modern biolipids and their preserved counterpart, geolipids and, therefore, prove the syngeneity of the data presented. This is especially important when presenting data from rocks and minerals that are extremely organically-lean. Modern contaminants can be introduced through collection of samples by lubricants, sunscreen, any type of plastic material, storage, and even during sample analysis (Brocks et al., 2008).

There are numerous characteristics that can provide evidence of syngeneity. One example is how the biomarkers are distributed throughout each sample and rock lithology (Grosjean and Logan, 2007). If samples contain similar distributions of biomarkers, this would suggest modern contaminants, or non-syngeneity (Brocks et al., 1999). For each sample in this study there are different distributions of biomarkers present in the chromatograms, suggesting syngeneity. Another example of syngeneity can be proven through the biomarker ratios calculated and reported previously. By using the OEP ratio or the Pr/nC<sub>17</sub>, Ph/nC<sub>18</sub> cross – plot (Figure 4.1), samples that have different biological input are considered syngeneic, while a non-syngeneic sample would have biological inputs from the same source. This is due to the fact that samples with the same source of biological input, most likely, were introduced during sample collection or sample analysis.

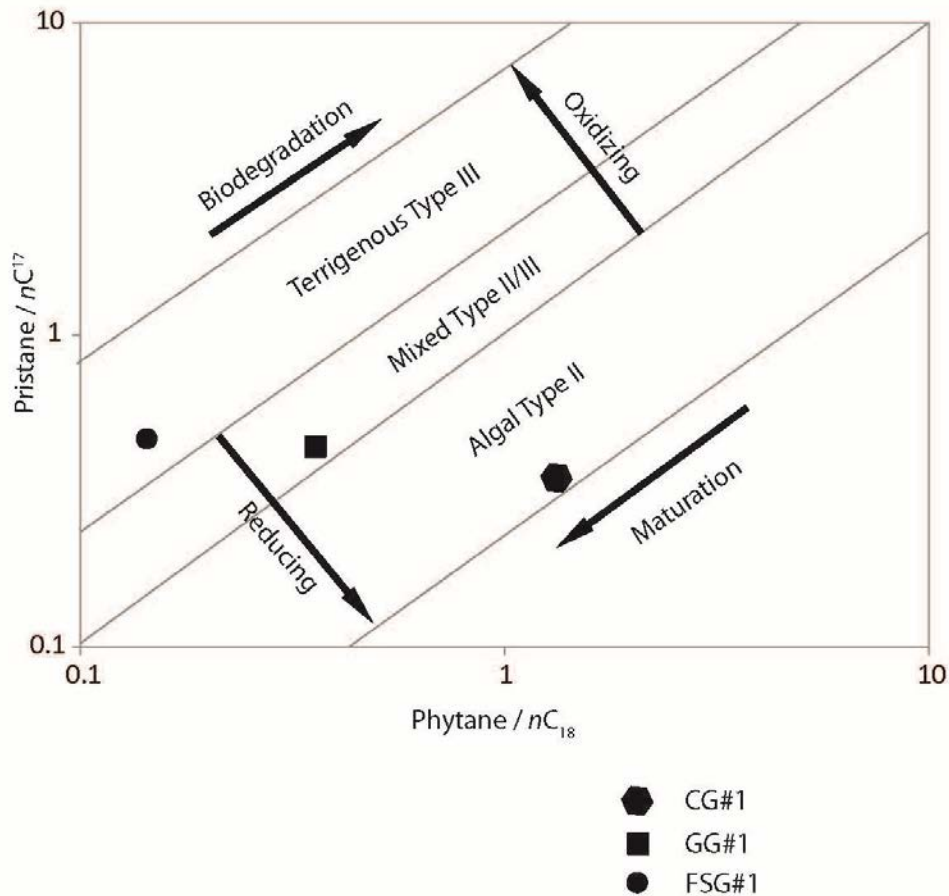


**Figure 4.1:** Pr/nC<sub>17</sub> vs. Ph/nC<sub>18</sub> cross – plot. Depicts the source of organic material from samples CG#1, GG#1, and FSG#1. (Modified from Shanmugam, 1985.)

A study by Brocks et al., (2003), looked at the syngeneity of molecular fossils in 2.78 – 2.45 billion year old rock from the Mount Bruce Supergroup, Pilbara Craton, in Western Australia. They tested the syngeneity of these molecular fossils by utilizing a series of procedures. A ratio of extract/blank was used in order to monitor contaminants introduced within the lab. This ratio was determined by creating blanks that were run to a set of five rock samples on a GC-FID and GC-MS-MS. If the ratio was < 20 the particular biomarker was considered non-syngeneic, and if it was > 20 it was syngeneic (Brocks et al., 2003). Also, comparisons were made between kerogen-rich and kerogen-poor rocks, bitumen maturity and thermal history of the

host rock and others. These comparisons were made in order to determine contamination introduced into the rock samples during collection, transport, rock powder preparations, or if there was any Phanerozoic contamination. Syngeneity of the kerogen-rich and kerogen-poor comparison was determined by kerogen-rich samples having a much higher amount of kerogen than the kerogen-poor blank rocks. Unfortunately, this type of comparison could not be performed in this study, however, other procedures such as those done in the Brocks et al., (2003) study, were able to be performed. For instance, the Brocks et al., (2003) study refers to each chromatogram displaying different distributions of biomarkers and that each sample has a thermal maturity consistent with the host rock, which is shown in figure 4.1 and in table 3.2. These two factors are important because as they help prove the syngeneity of the biomarkers.

In summary, the biomarkers presented in this study are indigenous to the host rock due to a number of factors. The data shown in the chromatograms and in the Pr/*n*C<sub>17</sub>, Ph/*n*C<sub>18</sub> cross – plot indicate the samples contain biological input from different sources. Comparisons made between the chromatograms of this study and of other studies show the syngeneity of the samples presented here. Also, the precautions that were taken during collection and lab procedures helped to diminish the possibility of contamination.

## **4.2 *n*-Alkane Interpretation**

The Dog Creek Formation contained samples DCSS#1, DC#2, and DC#3 that were previously described. DCSS#1 was the only sample that contained biomarkers, however, the chromatogram was noisy and showed low concentrations. With this some rough interpretations can be made of the *n*-alkanes that are present. In the DCSS#1 sample, the presence of short-chained *n*-alkanes and the lack of longer-chained *n*-alkanes suggests that this sample was subject

to higher forms of degradation. Often times long-chained *n*-alkanes can be degraded to form short-chained *n*-alkanes, but is not necessarily always the case (Peters et al., 2005a). This would coincide with the possibility of this sample containing or having remnants of long-chained *n*-alkanes as discussed in the results section. Another interpretation that can be made is from the most abundant peak of *n*C<sub>17</sub>. This indicated the organic matter present originated from an algae in a lacustrine or marine origin (Peters et al., 2005a). Due to the more recent paleoenvironmental interpretation of the Nippewalla Group the likely scenario would be a lacustrine origin (Benison and Goldstein, 1999; Benison and Goldstein, 2001). The lack of *n*-alkanes in the DC#2 and DC#3 samples implies that either biomarkers were not preserved and were degraded in this rock or they were never present.

Samples CG#1 and GG#1 from the Blaine Formation contained the highest range and abundance of *n*-alkanes. However, even though they are from the same formation they are interpreted differently due to the different abundances of the *n*-alkanes resulting in different ratio values. The CG#1 sample had values of 1.19, 0.27, 0.36, and 1.33 for the OEP, Pr/Ph, Pr/*n*C<sub>17</sub>, and Ph/*n*C<sub>18</sub> ratios respectively. OEP ratio values of approximately one are not very useful. However, it has a slight odd predominance, which could indicate higher-plant input from a terrigenous source. The Pr/Ph ratio value indicates the sample was deposited under anoxic conditions in a hypersaline environment. A cross-plot can be created from the Pr/*n*C<sub>17</sub> and Ph/*n*C<sub>18</sub> ratios (Figure 4.1) to depict the type of kerogen these biomarkers originated from. There are three main types of kerogen: I, II, and III. Type I is oil prone and typically consists of freshwater algae that forms in anoxic, organic-rich, shallow-water lacustrine environments (Killops and Killops, 2005). Type II is also oil prone and can be formed in any environment mostly from phytoplankton and higher plant material. Type III kerogen is more gas prone and

forms in terrigenous environments from vascular plants and other plant debris (Killops and Killops, 2005; Peters et al., 2005b). The CG#1 sample plots in the algal type II area. This is interpreted as being in a reducing environment with high maturation and consists mainly of algal type II kerogen on the Pr/*n*C<sub>17</sub> and Ph/*n*C<sub>18</sub> cross-plot. Overall the CG#1 sample can roughly be interpreted as being deposited under anoxic hypersaline conditions, with higher-plant input from a terrigenous source and algal type II kerogen.

For the GG#1 sample ratios were 1.49, 6.71, 0.43, and 0.36 for the OEP, Pr/Ph, Pr/*n*C<sub>17</sub>, and Ph/*n*C<sub>18</sub> ratios respectively. The OEP ratio for this sample suggests low thermal maturity as it is significantly greater than 1, in contrast to the CG#1 sample being interpreted as thermally mature. The Pr/Ph ratio is extremely high in this sample and is interpreted to reflect oxic conditions with terrigenous organic matter. The reason for the high ratio of Pr/Ph in this sample could be due to the co-elution of Pr with *n*C<sub>17</sub>. As for the Pr/*n*C<sub>17</sub> and Ph/*n*C<sub>18</sub> ratios, they were again plotted on the cross-plot, which indicated the organic matter in this sample is a mixed type II and III kerogen, with moderate reducing and oxidizing conditions. As a whole, this sample is interpreted to have low thermal maturity, oxic conditions, and terrigenous organic matter, along with a mixed type II and III kerogen.

The FSG#1 sample from the Flowerpot Shale Formation was the only sample that contained identifiable n-alkanes from which ratios were calculated. The ratio values calculated are 0.95, 4.33, 0.46, and 0.14, again for the OEP, Pr/Ph, Pr/*n*C<sub>17</sub>, and Ph/*n*C<sub>18</sub> ratios respectively. For the OEP ratio of 0.95, which is approximately one, there is not a clear odd over even predominance. This does suggest, however, that the sample is thermally mature and could originate from a hypersaline environment (Peters et al., 2005a). The Pr/Ph ratio of 4.33 is relatively high and indicates oxic conditions with terrigenous organic matter input. The cross-

plot of the  $Pr/nC_{17}$  and  $Ph/nC_{18}$  indicates that this sample is of terrigenous type III kerogen in an oxidative environment that is thermally mature. In summary this sample is thermally mature with terrigenous organic matter and type III kerogen input, in an oxic hypersaline environment.

The CG#1, GG#1 and FSG#1 samples were organic-lean and showed low concentrations of biomarkers. Due to this, the conclusions based on these samples should be treated with caution, as their accuracy may be questionable.

### 4.3 Hopane Interpretation

The hopanes were only present in the CG#1, GG#1, and the FGS#1 samples. However, hopane ratios for the GG#1 sample were not able to be calculated, as this sample did not contain the proper hopanes,  $C_{29} - C_{31}$ , nor Ts and Tm, needed for the formulas. Ratio values for the CG#1 sample are 1.27, 1.01, and 0.53 for the  $C_{29}/C_{30}$ ,  $C_{31}/C_{30}$ , and the Ts/Tm ratios, respectively. The  $C_{29}/C_{30}$  ratio value of 1.27 indicates this sample is characteristic of organic-rich carbonates or evaporites (Connan et al., 1986; Roushdy et al., 2010). A value of 1.01 for the  $C_{31}/C_{30}$  ratio indicates a marine source rock. The ratio Ts/Tm with a value of 0.53 indicates hypersaline conditions (Elfadly et al., 2016; Roushdy et al., 2010). The  $C_{31}/C_{30}$  ratio conflicts with the OEP ratio, which indicates a terrigenous source of organic matter. However, due to the fact that all other ratios point towards a freshwater or hypersaline source of organic matter, the  $C_{31}/C_{30}$  ratio may be proven to be inaccurate or an outlier.

The FGS#1 sample contained ratio values of 0.83, 0.48, and 1.03 for the  $C_{29}/C_{30}$ ,  $C_{31}/C_{30}$  and the Ts/Tm ratios, respectively. The  $C_{29}/C_{30}$  ratio value of 0.83 again represents organic-rich carbonates or evaporites and in this case, it would be evaporites. A  $C_{31}/C_{30}$  ratio value of 0.48 indicates marine source rock. However, other ratios indicate this environment is a

freshwater environment. One hypothesis as to why this ratio value indicates a marine source rock could be because it is interpreted as a hypersaline environment, which can give similar readings to a marine environment. The Ts/Tm ratio value of 1.03 indicates hypersaline conditions. This is because Ts is in greater quantities due to oxic conditions and the presence of shale (Peters et al., 2005a).

Even though some of the ratio values for these two samples contradict the *n*-alkane values, the majority of them points towards a hypersaline or evaporative environment, with terrigenous input of organic matter. This interpretation, and with the presence of gypsum, coincides with the current interpretation of the Nippewalla Group to be of hypersaline conditions.

Other *n*-alkane and hopane ratios indicate oxic conditions, as was the Nippewalla Group during the Permian. The ratios that do not indicate oxic conditions can be explained by microenvironments and/or fluid inclusions. As these two factors can play an important role in the preservation of organic matter.

#### **4.4 Geochemistry of the Nippewalla Group**

Biomarkers are a useful tool and can be used as an aid to better understand and interpret paleoenvironments. However, biomarkers are not always present and when they are it may be unique conditions as to which they were preserved, for example in fluid inclusions or microenvironments. As discussed previously the geochemistry of the Nippewalla Group is similar to that which has been hypothesized to prevent the preservation of biomarkers or any trace of chemical life will not be preserved (Sumner, 2004). Most of the lack of preservation potential is based on the fact of the high percentage of hematite present. This mineral forms

under oxidizing conditions, which in turn are detrimental to the preservation of biomarkers. In fact, Sumner 2004 illustrates that when hematite is in its most stable phase biomarkers are more likely to be oxidized than preserved. In the Nippewalla Group, however, it seems other factors may be at play and the actual geochemistry of the oxidizing environment is bypassed through the gypsum. These factors include microenvironments and fluid inclusions.

#### **4.5 Microenvironments**

Microenvironments are environments that are smaller and differ from the surrounding or dominating environment. They are separated from the dominating environment, or macroenvironment, usually by contrasting differences in geochemistry or geobiology (Didyk et al., 1978; May, 2013). A microenvironment can preserve organic matter in otherwise deteriorating conditions, specifically oxic conditions (Didyk et al., 1978; Macquaker et al., 2010; May, 2013; Shanks and Reeder, 1993). There are multiple ways they can form in order to aid the preservation of the organic matter. One way is due to bacteria colonizing the surface of organic aggregates or pellets as they settle through the water column creating an anoxic environment (May, 2013). The bacteria actually protect the organic matter from being subject to outside sources of degradation. Microenvironments can also be contained within the organic matter itself (Macquaker et al., 2010). Macquaker et al., (2010) found that certain clay-rich pellets in the Jet Rock Member of the Whitby Mudstone Formation in northeast England lacked pyrite and organomineralic aggregates (marine snow), which, suggested that there was an internal microenvironment in these pellets that had anaerobic microbial processes that were not as intense as the surrounding environment, allowing for the better preservation of organic matter. These studies show that when oxic sediment is present there can still exist reducing microniches, within

the sediment, that is better capable of preserving organic matter (Didyk et al., 1978; Shanks and Reeder, 1993).

With the Nippewalla group being dominated by oxic sediment, microenvironments could be a key factor in the preservation of the organic matter detected. In this way, the geochemistry of the microenvironments was actually anoxic instead of oxic. This can also explain how some of the results of the ratios calculated were interpreted to be anoxic instead of the overall oxic conditions present at the time of deposition. One example of a ratio value that was interpreted to be an anoxic environment instead of an overall oxic environment was the Pr/Ph ratio for the CG#1 sample. This ratio value was 0.27 indicating hypersaline, anoxic conditions, instead of hypersaline oxic conditions. The presence of microenvironments could create an environment with hypersaline anoxic conditions, rendering the Pr/Ph ratio of 0.27 plausible. Another example could also be said for the Pr/ $nC_{17}$  and Ph/ $nC_{18}$  cross-plot of the CG#1 sample. This sample was interpreted to be algal type II kerogen in reducing conditions on the cross-plot due to the higher phytane and  $nC_{17}$  content detected. There are multiple factors that can explain this scenario. Two of them being that the majority of biomarkers were detected in the gypsum of the Blaine Formation, which has been interpreted to have formed under hypersaline conditions. If the waters were supersaturated with the mineralogical constituents of gypsum and anhydrite it is possible that as these minerals grew, they could have absorbed the organic matter and incorporated it into their crystal lattice or provided a barrier to the outside oxic environment affectively preserving it. This could also explain the biomarkers detected in the Flowerpot Shale Formation and Dog Creek Formation. Two samples from the Flowerpot Shale and one sample from the Dog Creek formation contained biomarkers. The two samples of the Flowerpot Shale, SP#1 and FSG#1, both contained gypsum or was composed entirely of gypsum explaining how

biomarkers could have been preserved in these samples. The DCSS#1 of the Dog Creek Formation, however, was made up of oxidized fine-grained sandstone. With the minor amount of biomarkers detected in this sample it is possible there was either a minute amount of gypsum within the sample or there was another kind of microenvironment taking place.

#### **4.6 Fluid Inclusions**

Given the two studies mentioned in section 1.4, it is likely that some form of organic matter is entrapped in the fluid inclusions identified in the samples of this study. Evidence for the fluid inclusions to contain organic matter could be provided by Raman spectroscopy and/or fluorescence. However, problems can arise from Raman spectroscopy on gypsum. Gypsum is a strong Raman scatterer at certain wavelengths, meaning it emits a high Raman signature that obscures the Raman data of the fluid inclusions, in affect making it difficult to interpret the actual signature of the fluid inclusions (Osterrothová and Jehlička, 2011). The epoxy used to make the gypsum thin sections was also a strong Raman scatterer and for these reasons Raman spectroscopy was not performed in this study. A very small percentage of fluid inclusions did fluoresce, however, indicating possible organic matter (Figure 3.8). Also, fluid inclusions could explain the low TOC content detected in each sample as the fluid inclusions would be destroyed when the samples were powdered in order to obtain TOC analysis.

Even though not all of the fluid inclusions in this study were of primary origin the presence of them is important. This is especially due to the potential of some fluid inclusions containing organic matter, displayed by the slight fluorescence shown in figure 3.8. As this shows that fluid inclusions in general could entrap organic matter and that the geochemistry of

the area is bypassed by these fluid inclusions as they create another barrier to the overall oxic environment, similar to the microenvironments.

#### **4.7 Mars**

The preservation of biomarkers in the Nippewalla Group provides evidence of the potential for preservation of biomarkers on Mars. The Nippewalla Group and Meridiani Planum on Mars, have similar mineralogy and sedimentology. The mineralogy on Mars has been found to include evaporites, iron oxides, jarosite, and other sulfate minerals (Benison, 2006; McLennan et al., 2005). The iron oxides, namely hematite, extend over a very large area of approximately 200,000 km<sup>2</sup> and the evaporites are contained within this area of Meridiani Planum (McLennan et al., 2005). Recent and future missions to Mars contain instruments designed to detect biomarkers. The question of whether hematite-rich siliciclastic beds and evaporites can preserve chemical signs of life is important, as these environments are common on Mars. Currently, NASA is in the process of identifying the landing site of the next rover mission, many of which are hematite- and sulfate-rich (Chen et al., 2017). Some scientists argue, however, the next rover mission should not land in a hematite- and sulfate-rich environment, based on the assumption there will be no biomarkers, or any sign of microbial life (Sumner, 2004).

If the biomarkers are preserved in the Nippewalla Group, however, then the idea is that they could have been preserved by the same processes on Mars as well. This would in turn indicate that there was once life on Mars as the biomarkers would have had to originate from a once living organism.

Microenvironments and fluid inclusions are the two main factors that could potentially preserve biomarkers on Mars. Although not all of the fluid inclusions in this study were of

primary origin, their presence is important, especially since the chance that they contain organic matter is possible due to the slight fluorescence in figure 3.8. This shows that the geochemistry of the area is bypassed by fluid inclusions and if this process can happen in the Nippewalla Group then hopefully it can happen on Mars as well. With the presence of these fluid inclusions this gives hope to the discovery of organic matter on Mars. Whether the fluid inclusions are of primary or secondary origin is irrelevant as long as the organic matter that is trapped inside them is formed organically. If fluid inclusions were discovered in Martian rocks and contained original organic matter they would be proof of life on Mars, as the organic matter would have been trapped by the fluid inclusions during or shortly after the formation of the gypsum crystals. Microenvironments could play a key role in the preservation of biomarkers on Mars as well. The running water that once existed on the surface of Mars, may have provided the catalyst to preserving organic matter as it slowly evaporated creating gypsum crystals. These environmental conditions on Mars were similar to the paleoenvironmental conditions of the Nippewalla Group indicating the plausibility that microenvironments could exist on Mars. In this sense the gypsum discovered on Mars could create an inner anoxic environment, creating a barrier from the overall oxic conditions and, therefore, preserving any organic matter present during crystallization.

## CHAPTER FIVE: Conclusion

### 5.1 Conclusion

This study of the preservation potential of biomarkers in the Nippewalla Group of southern Kansas has provided evidence for the preservation of life in gypsum crystals associated with red-beds. Areas like these have been ignored due to their geochemistry and the likelihood of biomarkers not being preserved according to Sumner (2004). However, microenvironments and fluid inclusions are two factors that can effectively preserve biomarkers. As gypsum crystalizes, it can effectively engulf organic matter and, therefore, provide a barrier between the oxidizing macroenvironment and the inner microenvironment of the gypsum itself. This process of crystallization of gypsum can also obtain fluid and/or solid inclusions as the gypsum traps the fluid and/or solid inclusions preserving them. These two factors bypass the geochemistry and are able to preserve organic matter in an overall oxic environment. They also can explain why certain ratio values indicated an anoxic environment instead of an overall oxic one as the inner microenvironment was anoxic. This study has also illustrated a process that could help identify potential landing sites of future Mars rovers by classifying areas on Mars that could contain life, but has been overlooked due to the presence of hematite, for example Meridiani Planum. If the same processes that create microenvironments and fluid inclusions on Earth also exist on Mars, it is likely that biomarkers could be preserved in the gypsum of hematite rich areas. This provides a better understanding on how organic matter could be preserved on Mars. If microenvironments and fluid inclusions exist in the Nippewalla Group then there is a chance they could exist on Mars.

## References

- Baars, D. L., 1990, Permian chronostratigraphy in Kansas: *Geology*, v. 18, no. 8, p. 687-690.
- Benison, K., 1997, Acid water deposition and diagenesis in Permian red bed-hosted evaporites, midcontinent, United States of America, ProQuest Dissertations Publishing.
- Benison, K., 2013, Acid Saline Fluid Inclusions: examples from modern and Permian Extreme Lake Systems.
- Benison, K. C., and Goldstein, R. H., 2001, Evaporites and siliciclastics of the Permian Nippewalla Group of Kansas, USA: a case for non-marine deposition in saline lakes and saline pans: *Sedimentology*, v. 48, p. 165-188.
- Benison, K. C., Goldstein, R. H., Wopenka, B., Burruss, R. C., and Pasteris, J. D., 1998, Extremely acid Permian Lakes and ground waters in North America: *Nature*, v. 392, p. 911-913.
- Benison, K. C., Jagniecki, E. A., Edwards, T. B., Mormile, M. R., and Storrie-Lombardi, M. C., 2008, "Hairy blobs:" microbial suspects preserved in modern and ancient extremely acid lake evaporites: *Astrobiology*, v. 8, no. 4, p. 807-821.
- Benison, K. C., and Karmanocky, I. F. J., 2014, Could microorganisms be preserved in Mars gypsum? Insights from terrestrial examples: *Geology*, v. 42, no. 7, p. 615-618.
- Benison, K. C., Zambito, J. J., and Knapp, J., 2015, Contrasting Siliciclastic-Evaporite Strata In Subsurface and Outcrop: An Example From the Permian Nippewalla Group of Kansas, U.S.A: *Journal of Sedimentary Research*, v. 85, no. 6, p. 626-645.
- Bodnar, R. J., 2003, Introduction to fluid inclusions: Fluid inclusions: Analysis and interpretation, v. 32, p. 1-8.
- Brenna, J. T., Corso, T. N., Tobias, H. J., and Caimi, R. J., 1997, High-precision continuous-flow isotope ratio mass spectrometry: *Mass Spectrometry Reviews*, v. 16, no. 5, p. 227-258.
- Brocks, J. J., Buick, R., Logan, G. A., and Summons, R. E., 2003, Composition and syngeneity of molecular fossils from the 2.78 to 2.45 billion-year-old Mount Bruce Supergroup, Pilbara Craton, Western Australia: *Geochimica et Cosmochimica Acta*, v. 67, no. 22, p. 4289-4319.
- Brocks, J. J., Grosjean, E., and Logan, G. A., 2008, Assessing biomarker syngeneity using branched alkanes with quaternary carbon (BAQCs) and other plastic contaminants: *Geochimica et Cosmochimica Acta*, v. 72, no. 3, p. 871-888.
- Brocks, J. J., Logan, G. A., Buick, R., and Summons, R. E., 1999, Archean molecular fossils and the early rise of eukaryotes: *science*, v. 285, no. 5430, p. 1033-1036.

- Connan, J., Bouroulllec, J., Dessort, D., and Albrecht, P., 1986, The microbial input in carbonate-anhydrite facies of a sabkha palaeoenvironment from Guatemala: A molecular approach: *Organic Geochemistry*, v. 10, no. 1, p. 29-50.
- Conner, A. J., and Benison, K. C., 2013, Acidophilic halophilic microorganisms in fluid inclusions in halite from Lake Magic, Western Australia: *Astrobiology*, v. 13, no. 9, p. 850-860.
- Damste, J. S. S., ten Haven, H. L., De Leeuw, J. W., and Schenck, P. A., 1986, Organic geochemical studies of a Messinia evaporitic basin, northern Apennines (Italy)—II Isoprenoid and n-alkyl thiophenes and thiolanes: *Advances in Organic Geochemistry*, v. 10, p. 791-805.
- Didyk, B. M., Simoneit, B. R. T., Brassell, S. C., and Eglinton, G., 1978, Organic geochemical indicators of palaeoenvironmental conditions of sedimentation: *Nature*, v. 272, no. 5650, p. 216-222.
- Elfadly, A. A., Ahmed, O. E., and El Nady, M. M., 2016, Assessing of organic content in surface sediments of Suez Gulf, Egypt depending on normal alkanes, terpanes and steranes biological markers indicators: *Egyptian Journal of Petroleum*.
- Farrimond, P., Talbot, H. M., Watson, D. F., Schulz, L. K., and Wilhelms, A., 2004, Methylhopanoids: Molecular indicators of ancient bacteria and a petroleum correlation tool: *Geochimica et Cosmochimica Acta*, v. 68, no. 19, p. 3873-3882.
- Foster, T. M., Soreghan, G. S., Soreghan, M. J., Benison, K. C., and Elmore, R. D., 2014, Climatic and paleogeographic significance of eolian sediment in the Middle Permian Dog Creek Shale (Midcontinent U.S.): *Palaeogeography, Palaeoclimatology, Palaeoecology*, v. 402, p. 12-29.
- Gelpi, E., Schneider, H., Mann, J., and Oró, J., 1970, Hydrocarbons of geochemical significance in microscopic algae: *Phytochemistry*, v. 9, no. 3, p. 603-612.
- Giles, J. M., Soreghan, M. J., Benison, K. C., Soreghan, G. S., and Hasiotis, S. T., 2013, Lakes, Loess, and Paleosols In the Permian Wellington Formation of Oklahoma, U.S.A.: Implications For Paleoclimate and Paleogeography of the Midcontinent: *Journal of Sedimentary Research*, v. 83, no. 10, p. 825-846.
- Goldstein, R. H., and Reynolds, T. J., 1994, Fluid inclusion petrography.
- Grosjean, E., and Logan, G. A., 2007, Incorporation of organic contaminants into geochemical samples and an assessment of potential sources: Examples from Geoscience Australia marine survey S282: *Organic Geochemistry*, v. 38, no. 6, p. 853-869.
- Holdoway, K. A., 1978, Deposition of evaporites and red beds of the Nippewalla Group, Permian, Western Kansas: *Kansas Geological Survey Bulletin*, v. 215.

- Jahnke, L. L., Turk-Kubo, K. A., N. Parenteau, M., Green, S. J., Kubo, M. D. Y., Vogel, M., Summons, R. E., and Des Marais, D. J., 2014, Molecular and lipid biomarker analysis of a gypsum-hosted endoevaporitic microbial community: *Geobiology*, v. 12, no. 1, p. 62-82.
- Jarvie, D. M., 1991, Total Organic Carbon (TOC) Analysis: Chapter 11: GEOCHEMICAL METHODS AND EXPLORATION: AAPG, p. 113-118.
- Johnson, K., 1967, STRATIGRAPHY OF THE PERMIAN BLAINE FORMATION AND ASSOCIATED STRATA IN SOUTHWESTERN OKLAHOMA, ProQuest Dissertations Publishing.
- Killops, S. D., and Killops, V. J., 2005, Introduction to Organic Geochemistry: Malden, MA, Blackwell Pub., p. 30-70 & 166-245.
- Lowenstein, T., 2012, Microorganisms in Evaporites: Review of Modern Geomicrobiology, 117-139
- Macquaker, J. H. S., Keller, M. A., and Davies, S. J., 2010, Algal blooms and "Marine snow": Mechanisms that enhance preservation of organic carbon in ancient fine-grained sediments: *Journal of Sedimentary Research*, v. 80, no. 11-12, p. 934-942.
- Majhi, M. C., Behera, A. K., Kulshreshtha, N. M., Mahmooduzafar, D., Kumar, R., and Kumar, A., 2013, ExtremeDB: A Unified Web Repository of Extremophilic Archaea and Bacteria: *PLoS One*, v. 8, no. 5.
- May, J. A., 2013, The Sedimentology of Mudrocks: Organics, Organisms, and Occasional Occurrences, Unconventional Resources Technology Conference.
- Moldowan, J. M., Seifert, W. K., and Gallegos, E. J., 1985, Relationship between petroleum composition and depositional environment of petroleum source rocks: *AAPG bulletin*, v. 69, no. 8, p. 1255-1268.
- Newell, K. D., Watney, W. L., Cheng, W., and Brownrigg, R. L., 1989, Stratigraphic and spatial distribution of oil and gas production in Kansas.
- Onojake, M. C., Osuji, L., and Abrakasa, S., 2015, Source, depositional environment and maturity levels of some crude oils in southwest Niger Delta, Nigeria: *Chinese Journal of Geochemistry*, v. 34, no. 2, p. 224232.
- Osterrothová, K. and Jehlička, J., 2011, Feasibility of Raman Microspectroscopic Identification of Biomarkers Through Gypsum Crystals: *Spectrochimica Acta Part A: Molecular Biomolecular Spectroscopy*, v. 80, no. 1, p. 96-101.

- Peters, K. E., and Moldowan, J. M., 1991, Effects of source, thermal maturity, and biodegradation on the distribution and isomerization of homohopanes in petroleum: *Organic Geochemistry*, v. 17, no. 1, p. 47-61.
- Peters, K. E., Walters, C. C., and Moldowan, J. M., 2005a, *The Biomarker Guide: Biomarkers and Isotopes in Petroleum Exploration and Earth History Vol. 2*, New York, Cambridge University Press, v. 2.
- , 2005b, *The Biomarker Guide: Biomarkers and Isotopes in the Environment and Human History Vol. 1*, New York, Cambridge University Press, v. 1.
- Powell, T. G., and McKirdy, D. M., 1973, Relationship between Ratio of Pristane to Phytane, Crude Oil Composition and Geological Environment in Australia: *Nature*, no. 243, p. 37-39.
- Prahl, F., Hayes, J., and Xie, T.-M., 1992, Diploptene: an indicator of terrigenous organic carbon in Washington coastal sediments.
- Röper M. (1983) Fischer-Tropsch Synthesis. In: Keim W. (eds) *Catalysis in C1 Chemistry. Catalysis by Metal Complexes*, vol 4. Springer, Dordrecht
- Rothschild, L. J., and Mancinelli, R. L., 2001, Life in extreme environments: *Nature*, v. 409, no. 6823, p. 1092-1101.
- Roushdy, M., El Nady, M., Mostafa, Y., El Gendy, N. S., and Ali, H., 2010, Biomarkers characteristics of crude oils from some oilfields in the Gulf of Suez, Egypt: *Journal of American Science*, v. 6, no. 11, p. 911-925.
- Schafer, G., 2004, Extremophilic archaea and bacteria - Introduction: *J. Bioenerg. Biomembr.*, v. 36, no. 1, p. 3-4.
- Schopf, J. W., Farmer, J. D., Foster, I. S., Kudryavtsev, A. B., Gallardo, V. A., and Espinoza, C., 2012, Gypsum-permineralized microfossils and their relevance to the search for life on Mars: *Astrobiology*, v. 12, no. 7, p. 619-633.
- Shanks, A., and Reeder, M. L., 1993, Reducing microzones and sulfide production in marine snow, 43-47
- Soreghan, G. S., Benison, K. C., Foster, T. M., Zambito, J., and Soreghan, M. J., 2014, The paleoclimatic and geochronologic utility of coring red beds and evaporites: a case study from the RKB core (Permian, Kansas, USA): *International Journal of Earth Sciences*, v. 104, no. 6, p. 1589-1603.
- Sumner, D. Y., 2004, Poor preservation potential of organics in Meridiani Planum hematite-bearing sedimentary rocks: *Journal of Geophysical Research*, v. 109, no. 12, p. 1-9.

Sweet, A. C., Soreghan, G. S., Sweet, D. E., Soreghan, M. J., and Madden, A. S., 2013, Permian dust in Oklahoma: Source and origin for Middle Permian (Flowerpot-Blaine) redbeds in Western Tropical Pangaea: *Sedimentary Geology*, v. 284-285, p. 181-196.

Volkman, J. K., 1986, A review of sterol markers for marine and terrigenous organic matter: *Organic Geochemistry*, v. 9, no. 2, p. 83-99.

Welander, P. V., Coleman, M. L., Sessions, A. L., Summons, R. E., and Newman, D. K., 2010, Identification of a methylase required for 2-methylhopanoid production and implications for the interpretation of sedimentary hopanes.(EVOLUTION: GEOLOGY)(Author abstract)(Report): *Proceedings of the National Academy of Sciences of the United States*, v. 107, no. 19, p. 8537.